Astrophysical Sources of High Energy Radiation and Particles in the Era of CTA and ASTRO-H

Lukasz Stawarz (ISAS/JAXA)
Tadayuki Takahashi (ISAS/JAXA)
Yasunobu Uchiyama (KIPAC/SLAC)

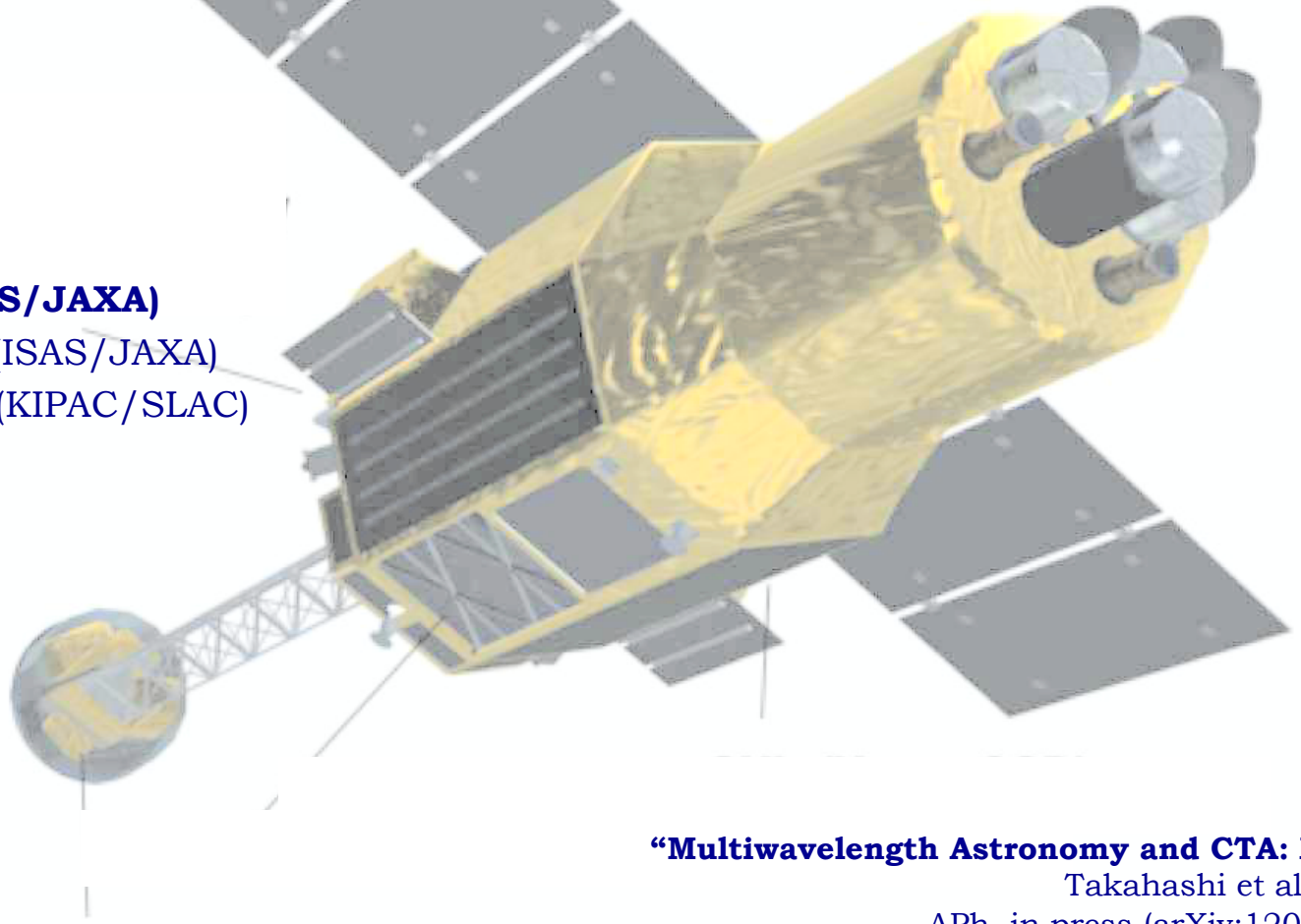

"Multiwavelength Astronomy and CTA: X-rays"
Takahashi et al., 2012,
APh, in press (arXiv:1205.2423)

Outline of the Talk

- **ASTRO-H**
- **Low-Power Blazars (BL Lacs)**
- **High-Power Blazars (FSRQs)**
- **Misaligned Blazars (Radio Galaxies)**
- **Radio-Quiet AGN (Seyferts)**
- **Clusters of Galaxies**
- **Summary: X-ray/γ-ray synergy**

ASTRO-H

ASTRO-H, to be launched in 2014, will carry the first focusing hard X-ray telescope with graded multilayer reflecting surface operating in the energy range 5-80 keV. In addition to the **Hard X-ray Imager**, ASTRO-H will carry two soft X-ray telescopes, one with a micro-calorimeter spectrometer array with excellent energy resolution (**Soft X-ray Spectrometer**), and the other with a large area CCD in their respective focal planes. In order to extend the energy coverage to the soft gamma-ray regime, the **Soft Gamma-ray Detector** will be implemented as a non-focusing detector covering the energy range 40-600 keV, and being capable of measuring polarization of bright (>10mCrab) sources.

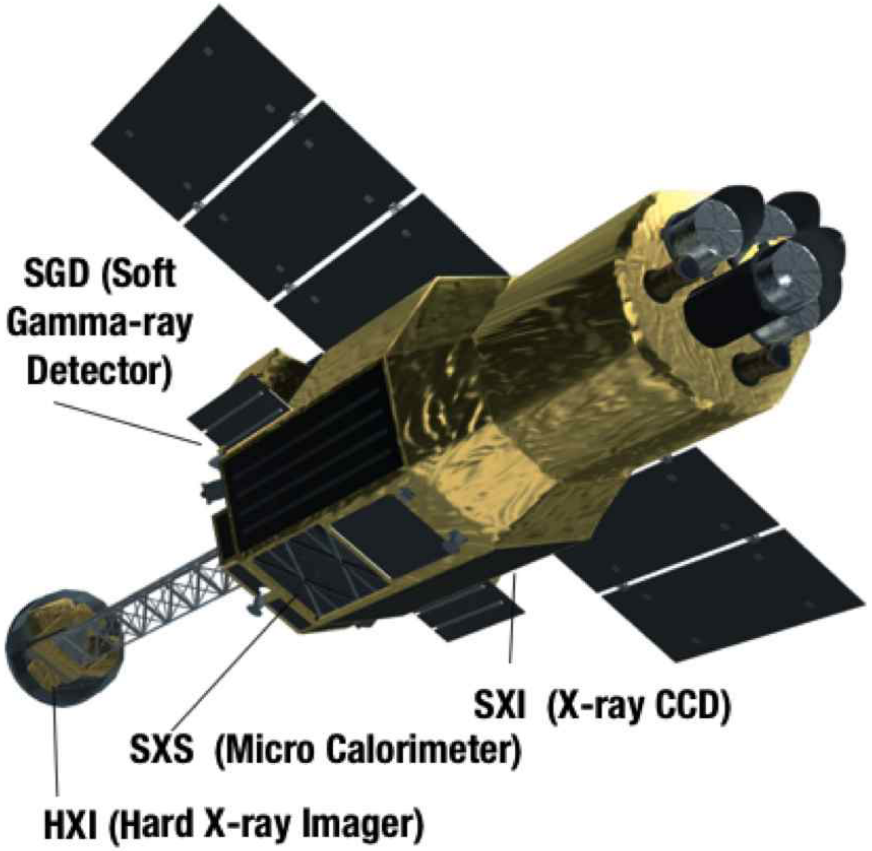

HXI & SGD

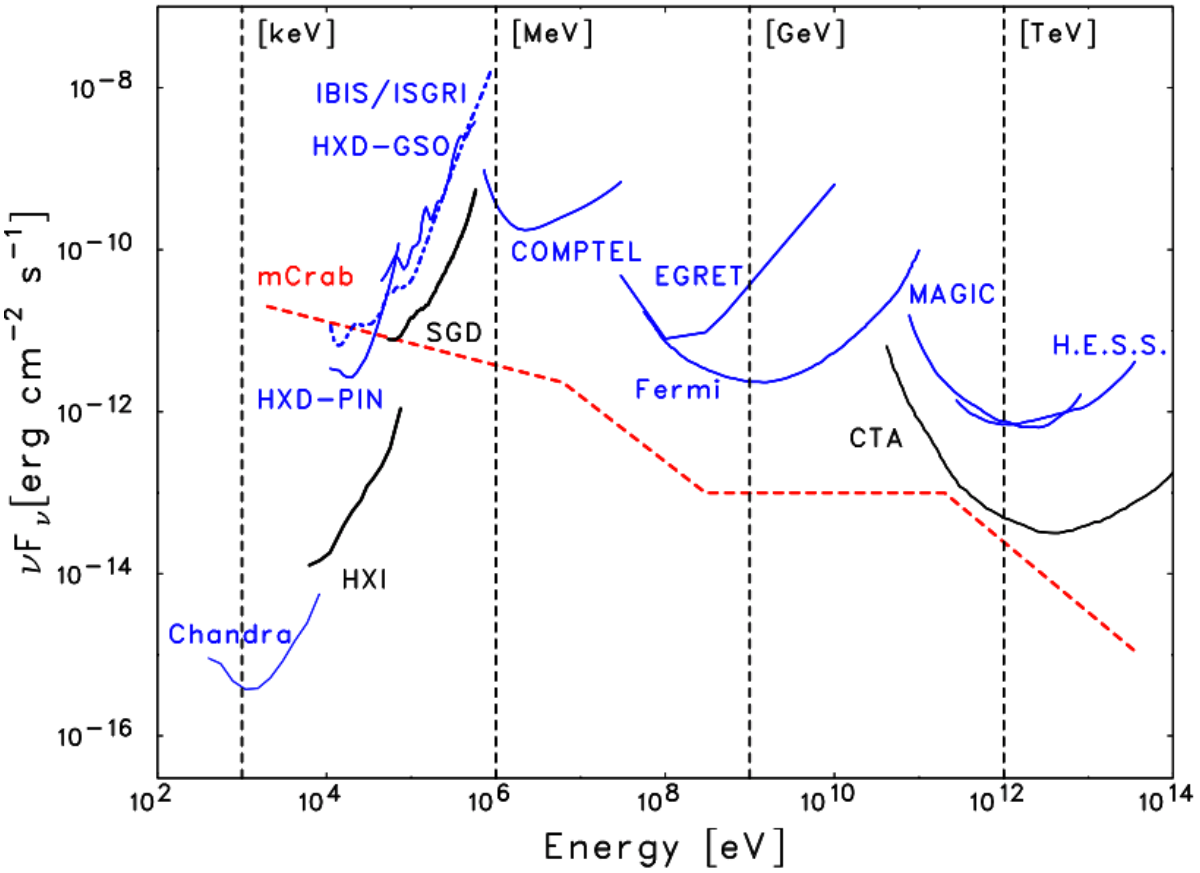

Chandra/ACIS-S, Suzaku/HXD (PIN & GSO), Integral/IBIS, ASTRO-H/HXI & SGD:
3σ sensitivity curves for 100 ks exposures; ΔE/E = 0.5.

CGRO/COMPTEL & EGRET: all-lifetime all-sky survey.

Fermi/LAT: pre-launch sensitivity for the 5σ detection limit at high Galactic latitudes with 0.25-decade ranges of energy in a one-year dataset.

MAGIC, H.E.S.S.: 5σ detection with >10 excess photons after 50h exposure.

CTA: simulated configuration C sensitivity curve for 50h exposure at a zenith angle of 20deg.

SXS

Imaging spectroscopy with an energy resolution <7 eV by the SXS of extended sources can reveal line broadening and Doppler shifts due to turbulent or bulk velocities of the X-ray emitting plasma, enabling the determination of the level of turbulent pressure support in clusters, supernova ejecta dispersal patterns, the structure of active galactic and starburst winds, and the spatially dependent abundance pattern in clusters and elliptical galaxies.

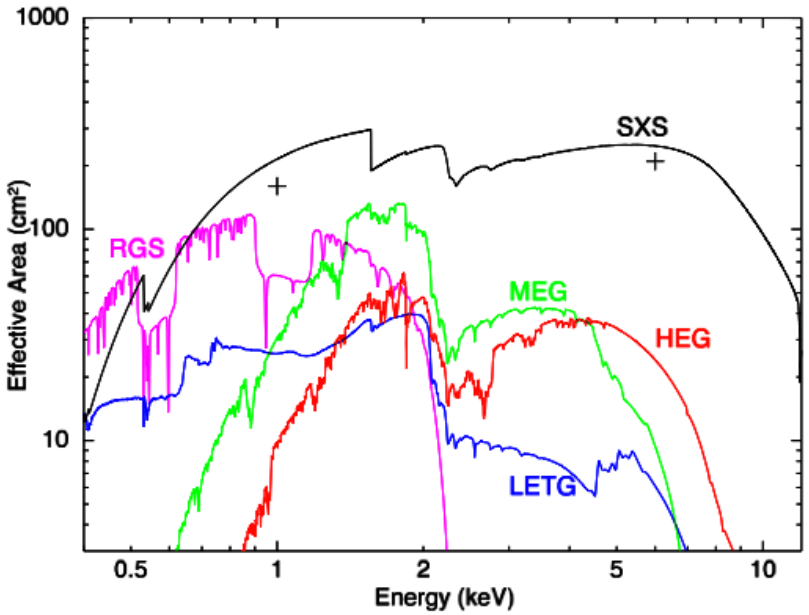

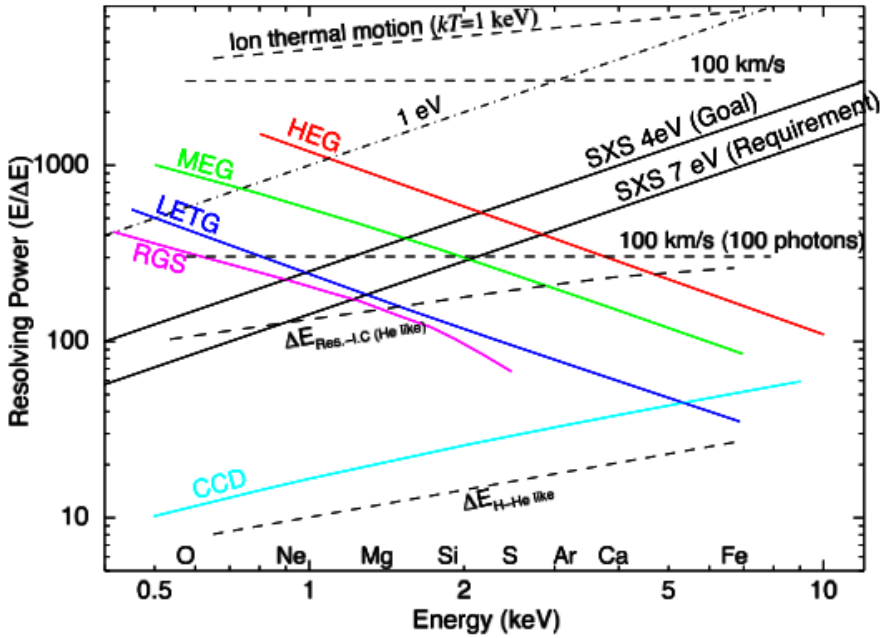

ASTRO-H/SXS
XMM/RGS (RGS-1 & RGS-2)
Chandra/LETG, MEG & HEG

The spectroscopic capability of X-ray micro-calorimeters is truly unique!

Hard X-ray Sky

- All-sky-survey by BAT onboard SWIFT resulted in the detection of 1092 sources (at the significance level of ≥4.8σ) in the 58-month accumulation of the data within the photon energy range 14-195 keV (Baumgartner et al. 2011). Majority of sources (730) have been identified with extragalactic objects, and in particular with AGN (627).

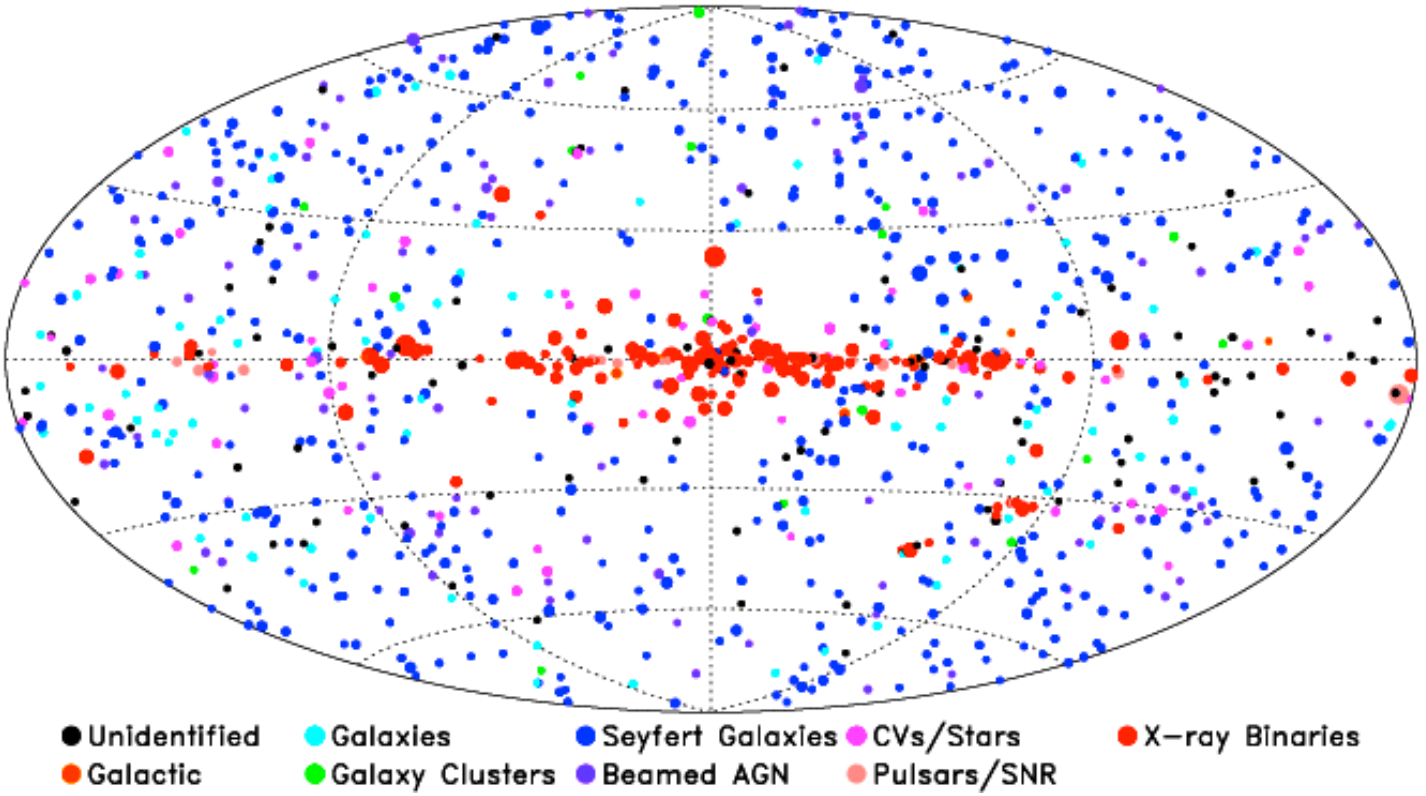

GeV Sky

- 2nd catalog of AGN detected by LAT ("2LAC", 24 months of data collected in scientific operation mode) includes 1016 gamma-ray sources located at high Galactic latitudes (|b|>10°) that are detected at high significance (≥5σ) and associated statistically with AGN (Ackermann et al. 2011).

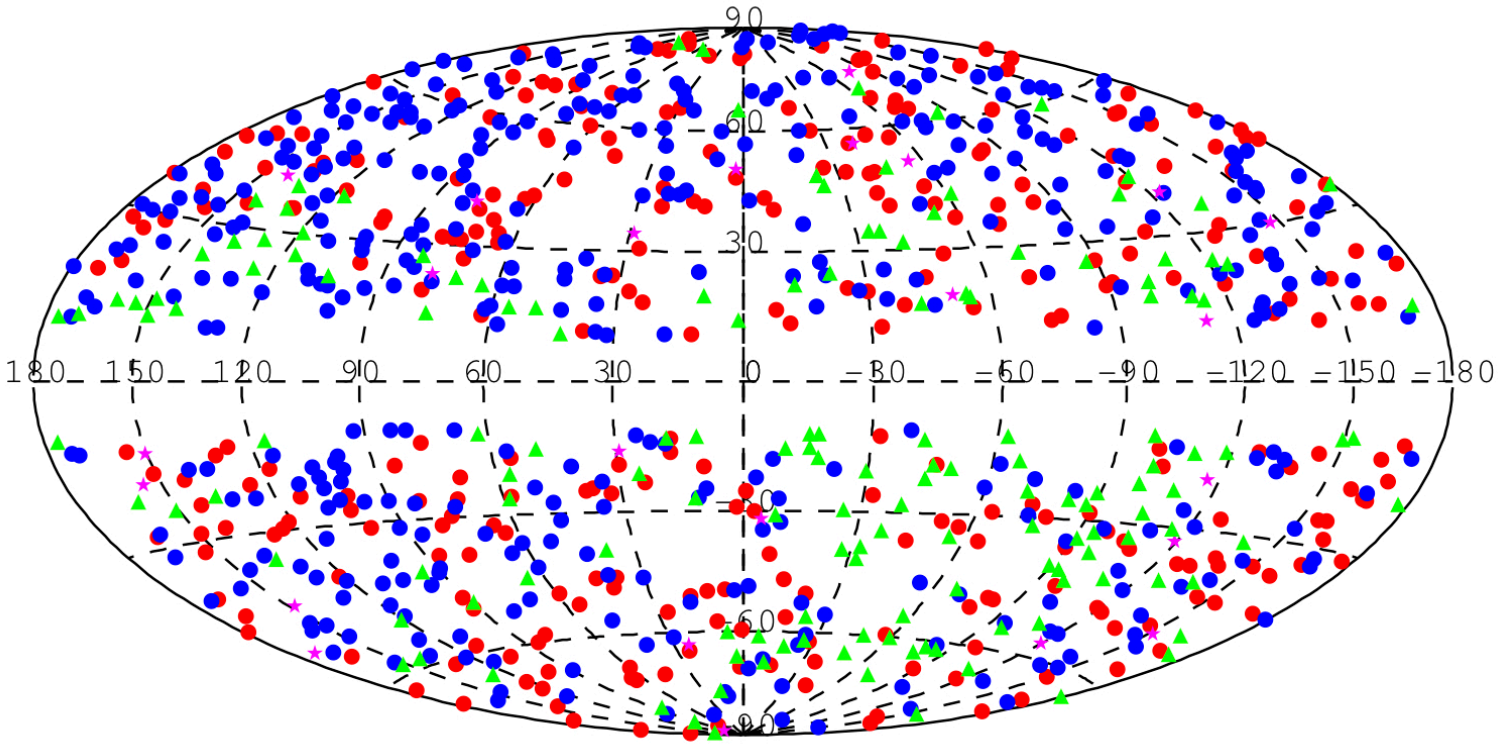

885 AGN in a "clean 2LAC sample" comprising 395 BL Lacs, 310 FSRQs, 22 AGN of other types, and 156 AGN of unknown types (to be compared with ~100 AGN, mostly FSRQs, associated with EGRET sources; Hartman et al. 1999).

TeV Sky

- The extragalactic TeV sky is dominated by blazars as well, with BL Lacs constituting majority of the detected sources. Most of the objects were discovered during the last decade thanks to the operation of modern Cherenkov Telescopes H.E.S.S., Magic, or VERITAS.

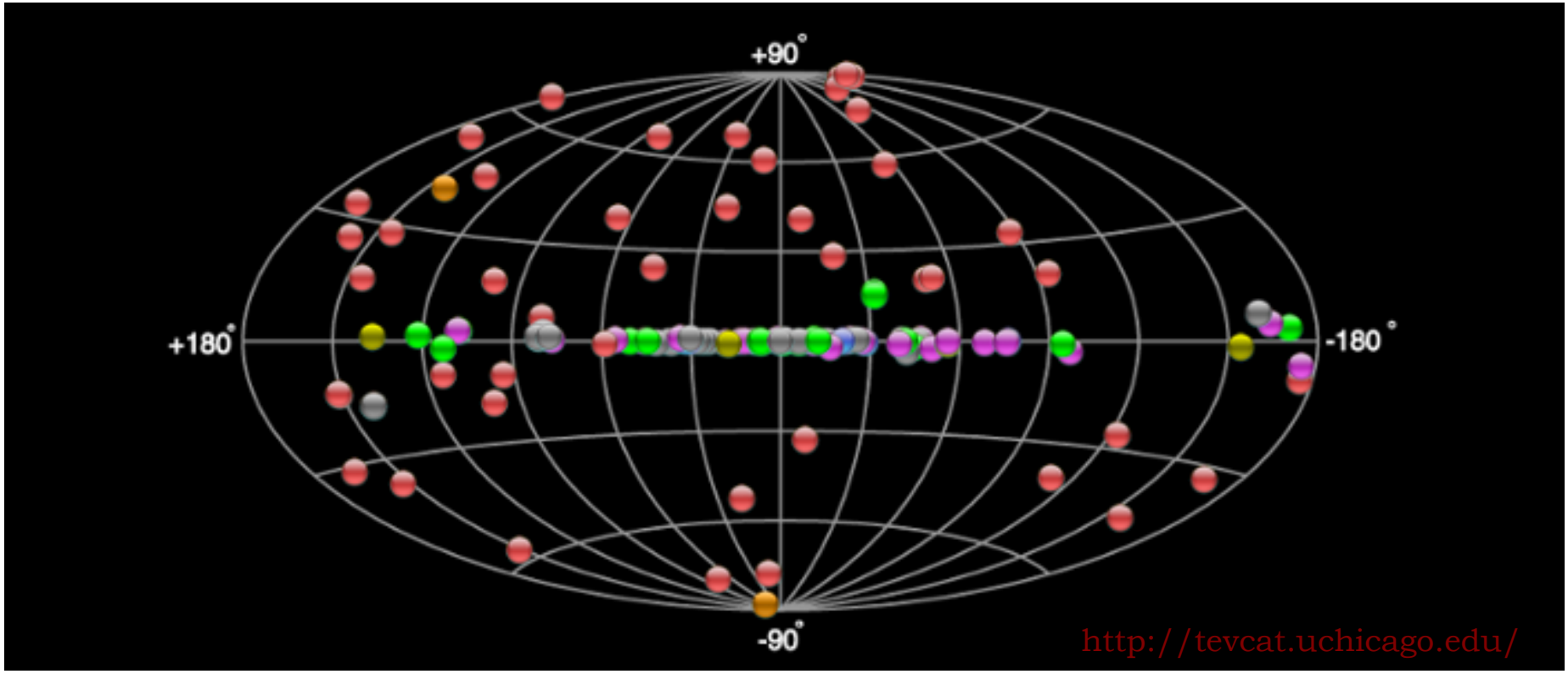

Much more AGN are expected to be detected in a near future with CTA!

Active Galactic Nuclei

AGN are established sources of a broad-band emission.

In non-blazar objects, IR emission is dominated by the circumnuclear dust, optical-to-UV emission by accretion disks, and X-ray emission by the accretion disk coronae.

In blazar sources, the entire radio-to-γ-ray continuum is due to the emission of relativistic jets. Rapid and large-amplitude variability of blazars points toward a very efficient and extremely rapid acceleration of the jet particles to ultrarelativistic energies, typically ascribed to shocks.

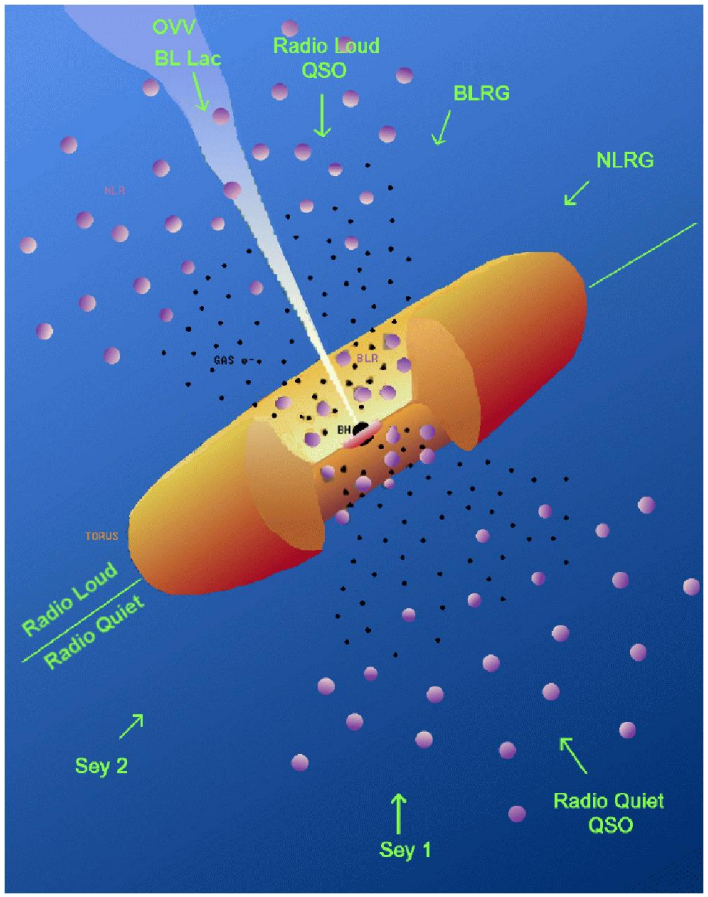

Urry & Padovani 1995

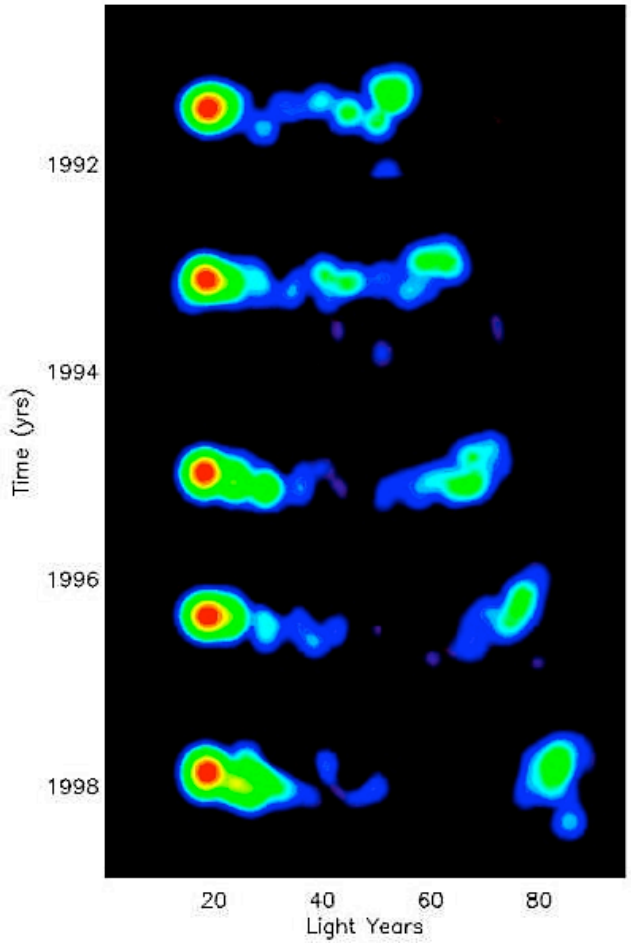

“Standard” Blazar Models

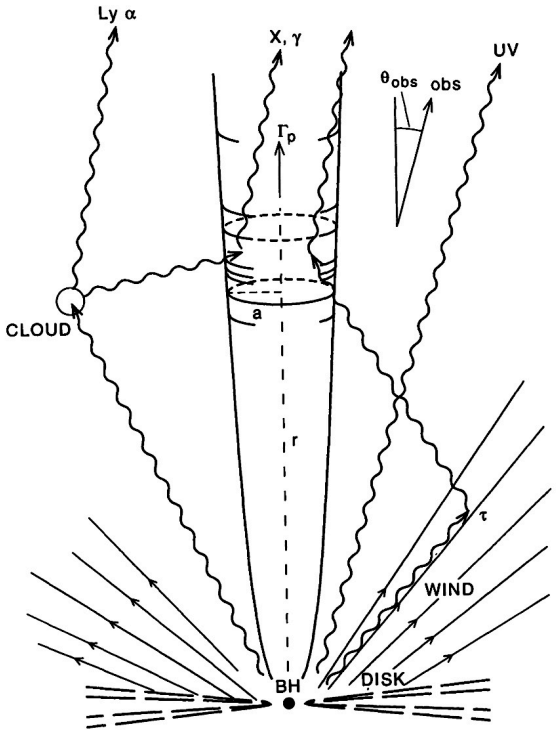

Sikora et al. 1994

High-power blazars: FSRQs (3C454.3)
Low-power blazars: BL Lacs (Mrk 421)

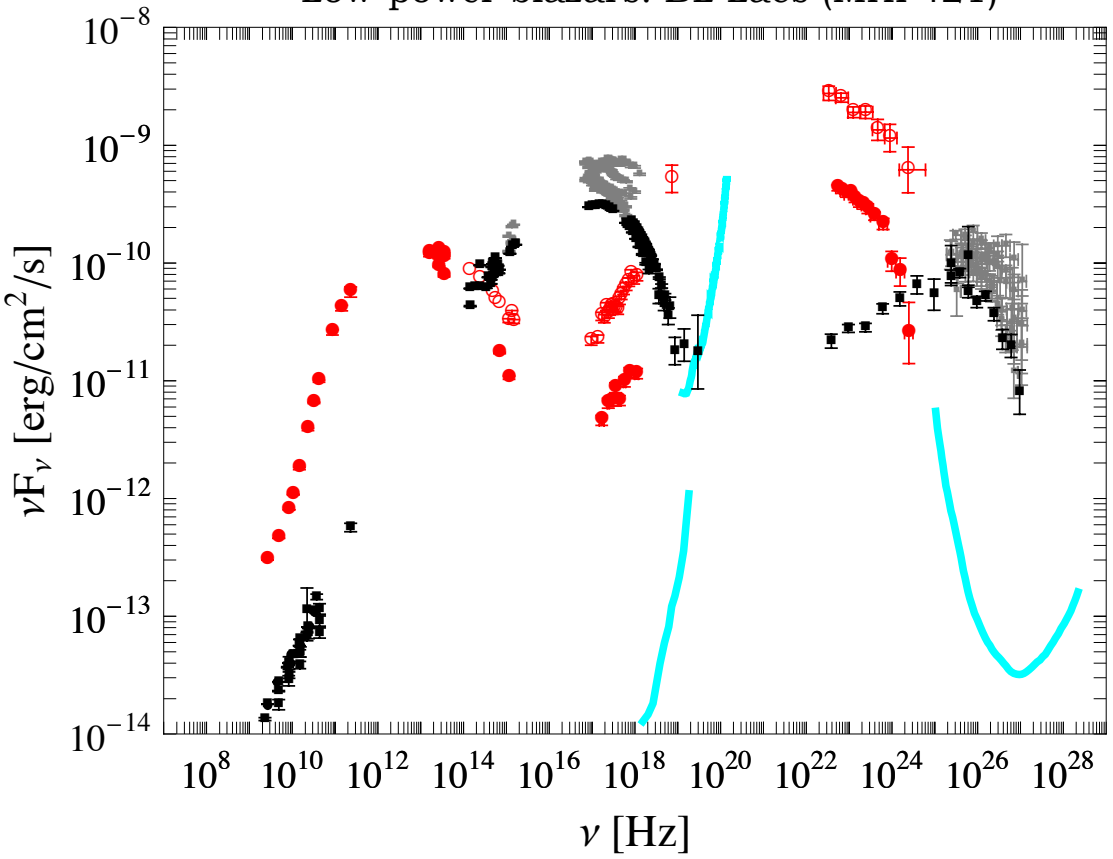

Single well-defined and homogeneous emission zone at $>10^2\,R_g \sim 10^{16}$ cm distances from the central SMBH – clearly a huge oversimplification, justified in the EGRET era, but not anymore.

Most of the radiatively dissipated power of blazars is emitted in either X-ray or γ-ray domains.

BL Lacs

The correlated variability in the X-ray and TeV bands established for many BL Lacs (e.g., Mrk 421) proves the inverse-Compton origin of the observed gamma-rays.

The exact correlation patterns emerging from detailed analysis revealed a picture which is much more complex than that expected in the "standard" models, assuming a single homogeneous emission zone and a simplified prescription for the shock acceleration of the radiating particles.

LS: it is not clear if more sophisticated models involving multiple or inhomogeneous emission zones are necessarily more realistic. The crucial problem seems to be related to hardly understood particle acceleration processes involved.

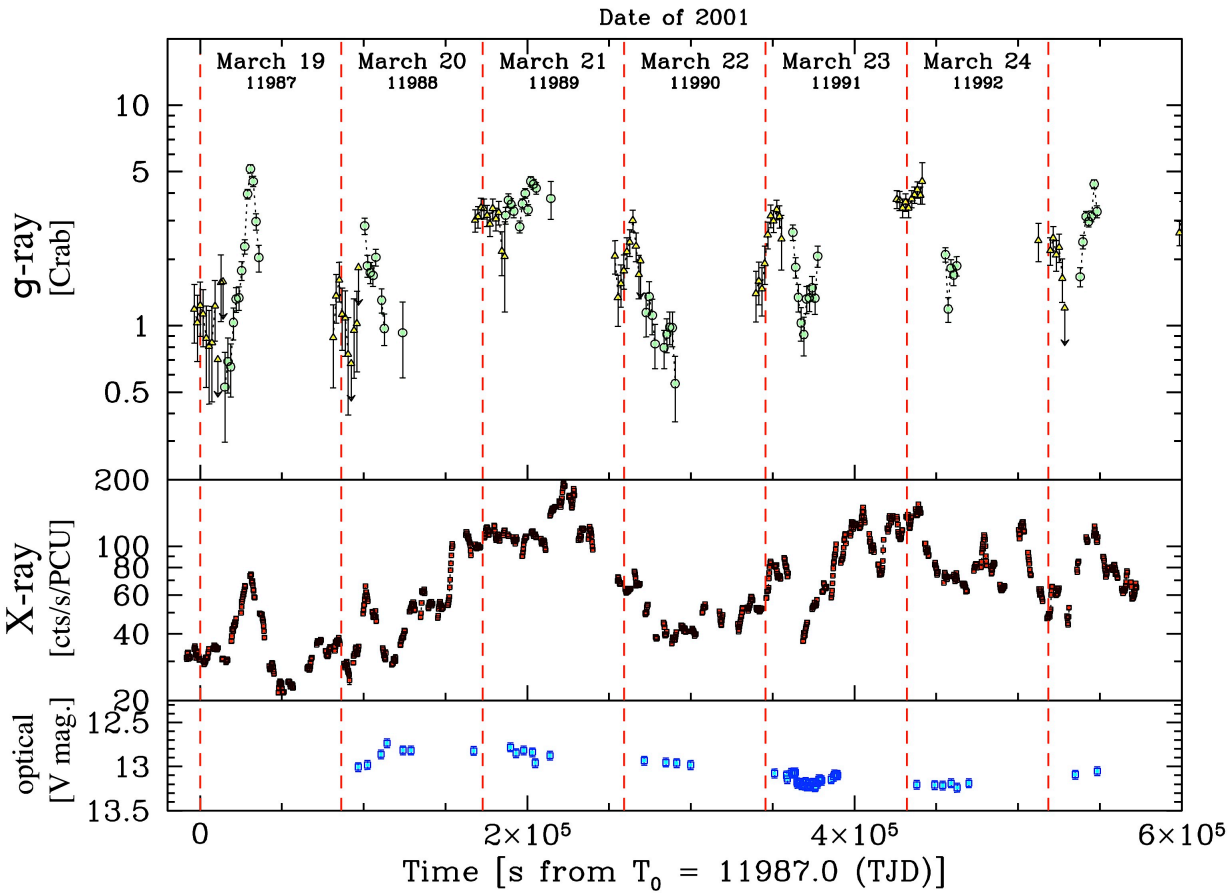

Fossati et al. 2008

Highest Energy Electrons

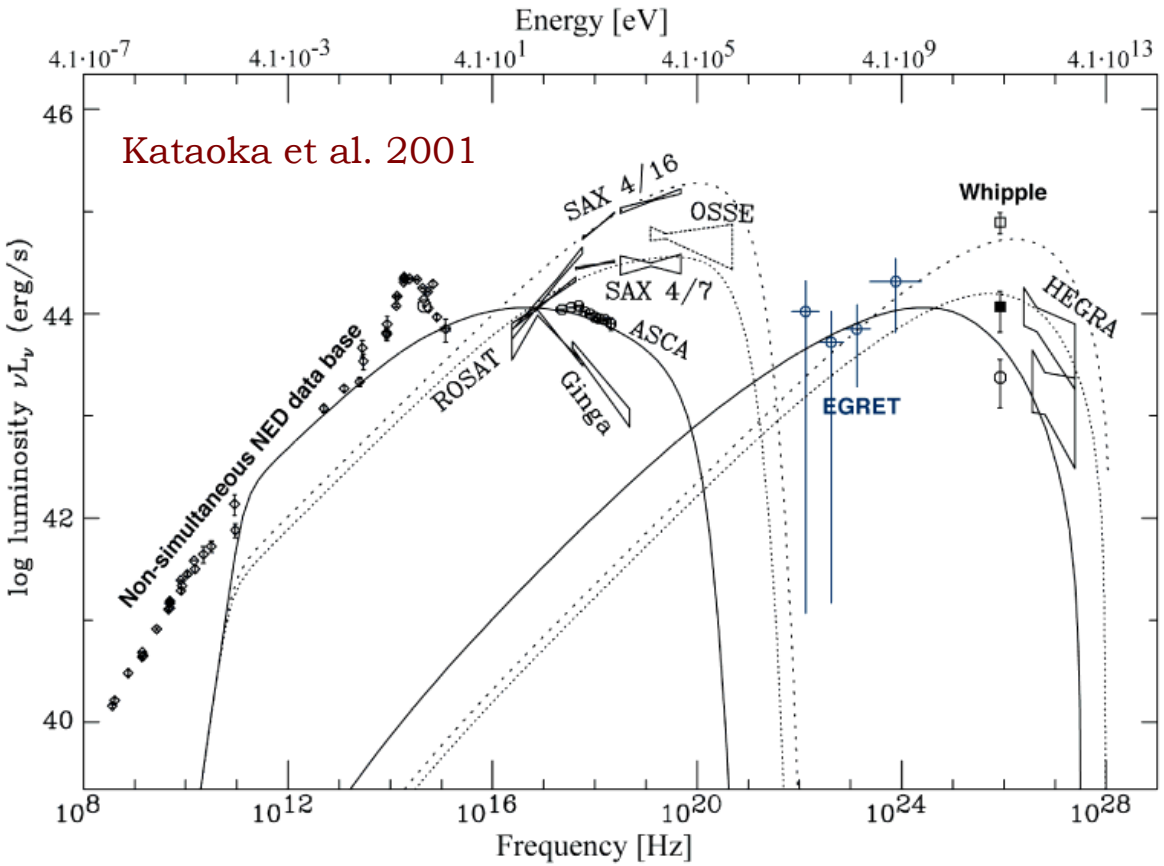

An exciting and unique possibility for constraining particle acceleration processes taking place in blazar jets is the detection of the polarization in hard X-rays by SGD during particularly strong flaring states of the brightest BL Lacs, like that of Mrk 501 in 1997 when the synchrotron continuum of the source extended up to the >100 keV photon energy range.

X-ray domain carries information regarding the >TeV energy electrons directly involved in shaping the gamma-ray properties of BL Lacs.

Instruments HXI and SGD onboard ASTRO-H will enable us, for the very first time, to track the spectral evolution of several bright BL Lacs above 10 keV photon energies in 100 ks (or even shorter) exposures.

MWL Campaigns

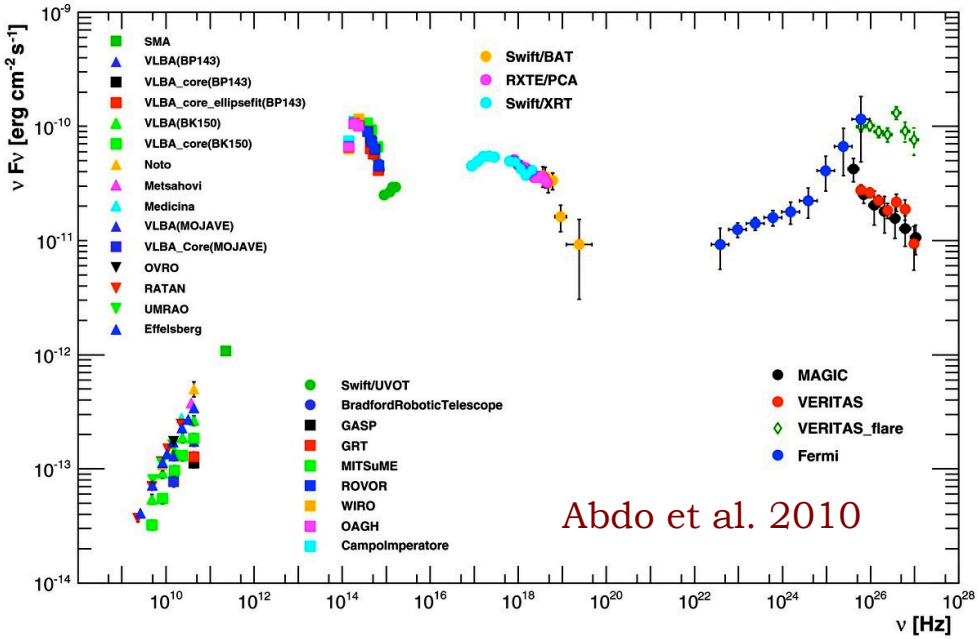

Abdo et al. 2010

Truly MWL and simultaneous observations of Mrk 501 with the best (up to date) spatial and temporal coverage (Abdo et al. 2010; CAs: Paneque & LS).

Hard X-rays: Swift/BAT
VHE γ-rays: MAGIC & VERITAS

Hard X-ray and soft gamma-ray regimes are the least explored!

"Typical" behavior of Mrk 501: only modest and rather long-timescale flux changes

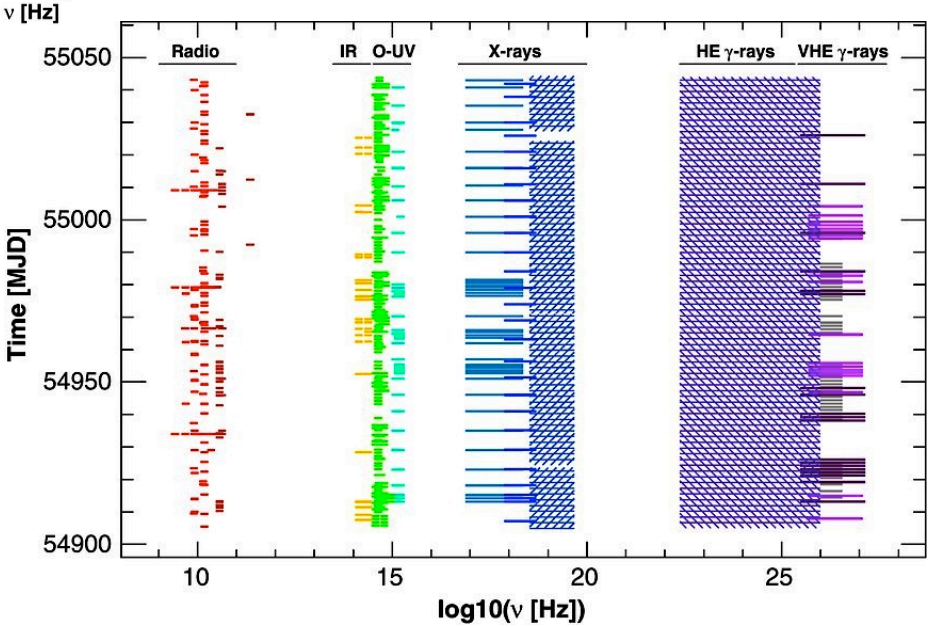

Ultrafast Variability

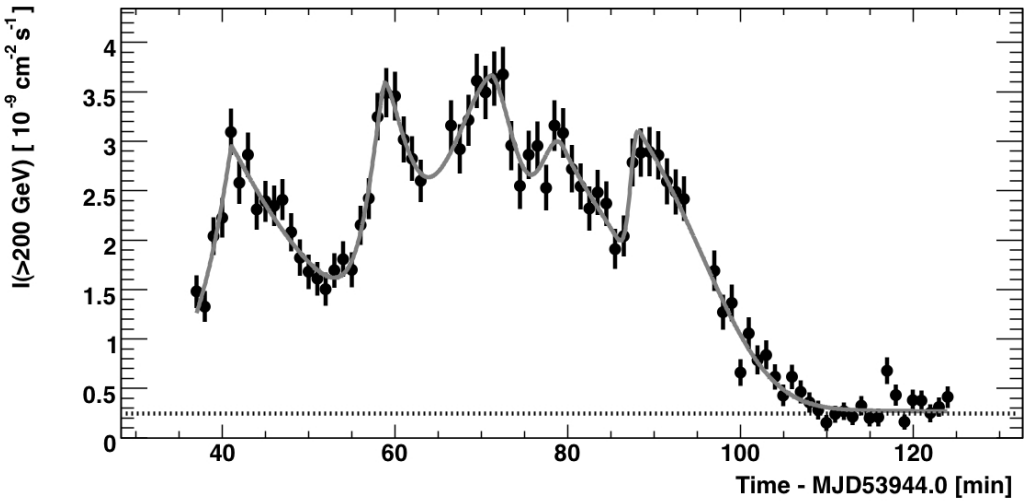

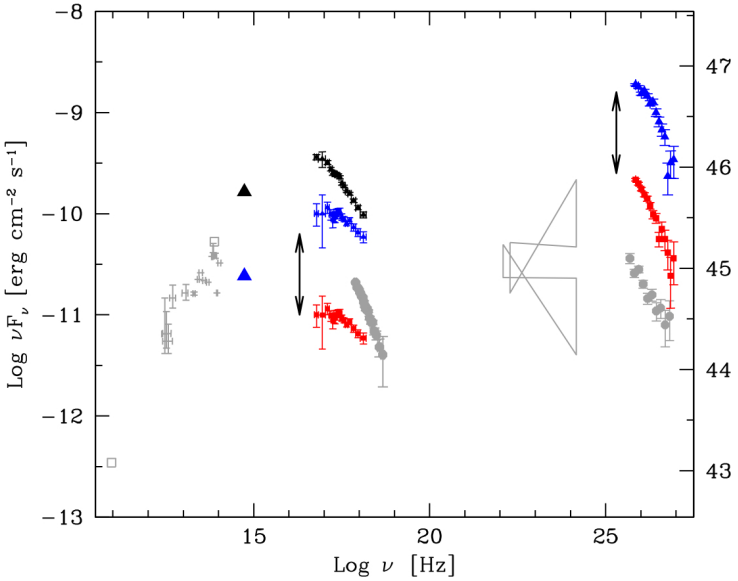

Variability in the TeV range for PKS 2155-304 is seen up to ~600 sec in the Fourier power spectrum, and well-resolved bursts varying on time scales of ~200 sec are observed. There are no strong indications for spectral variability within the data. The shortest observed flux doubling timescale, t_{var} ~ 200 s, implies linear size of the emitting region $R < c\, t_{var}\, \delta$. For the mass of the black hole $M_{BH} \sim 10^9\, M_{sun}$, this gives $R \sim (\delta/100) \times R_g$ suggesting that the blazar zone is located in the closest vicinity of the black hole, and that the whole outflow is already extremely relativistic thereby (Aharonian et al. 2007, 2009)

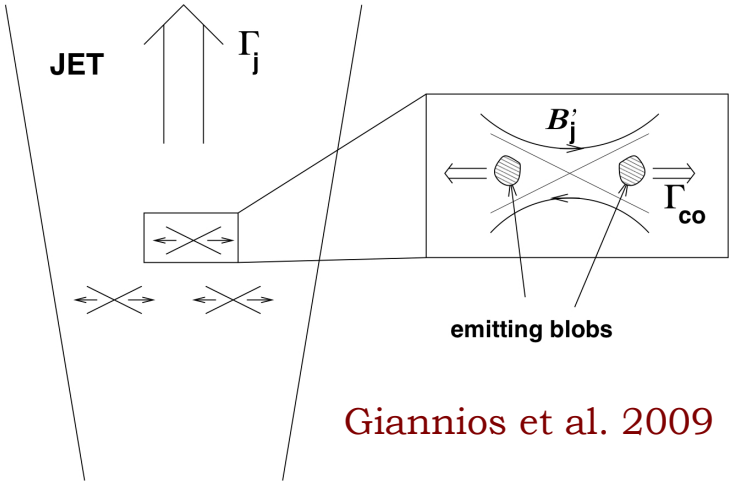

Giannios et al. 2009

FSRQs

In FSRQs the X-ray observations probe the low-energy segment of the high-energy emission component. This high-energy component dominates energetically over the synchrotron one, reaching apparent gamma-ray luminosities as large as ~10^{49} erg/s during the flaring states.

The low-energy tail of the high-energy emission components of FSRQs is produced via the IC process involving the lowest-energy electrons, down to the mildly-relativistic regime. **Hence these are the <u>combined</u> gamma-ray and X-ray observations which constrain the jet energetics in FSRQs.**

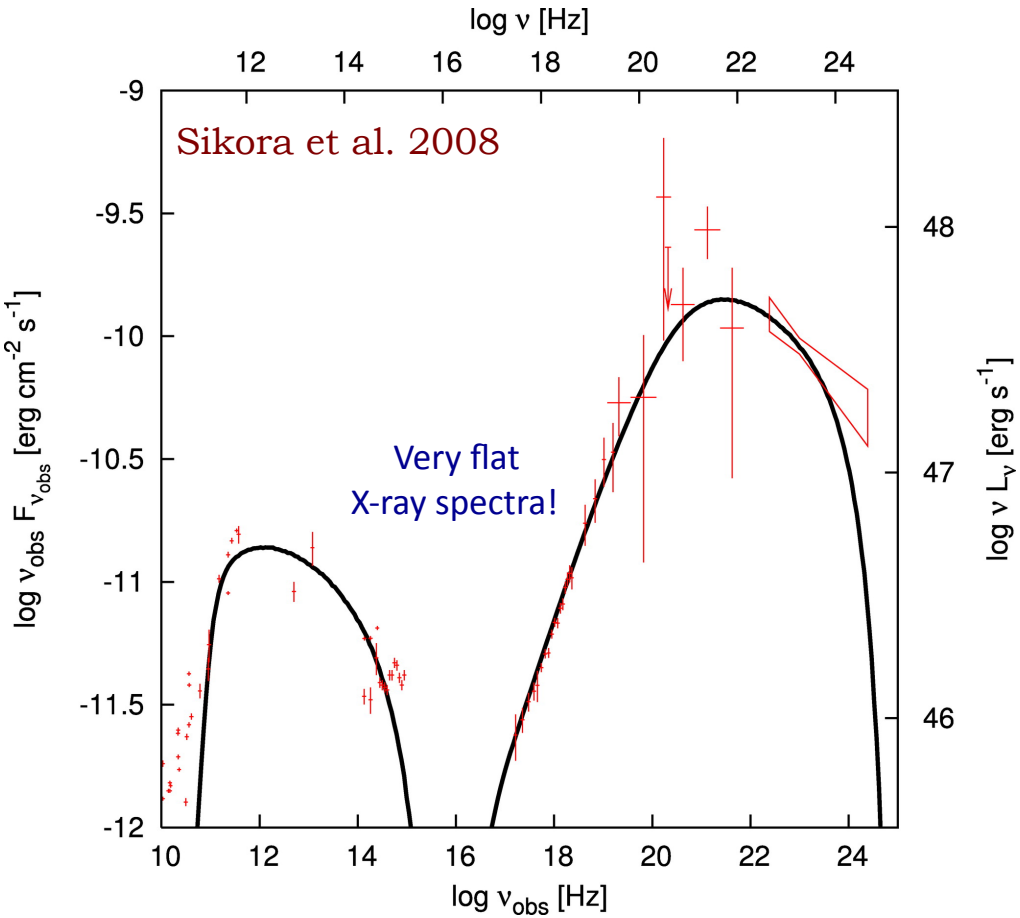

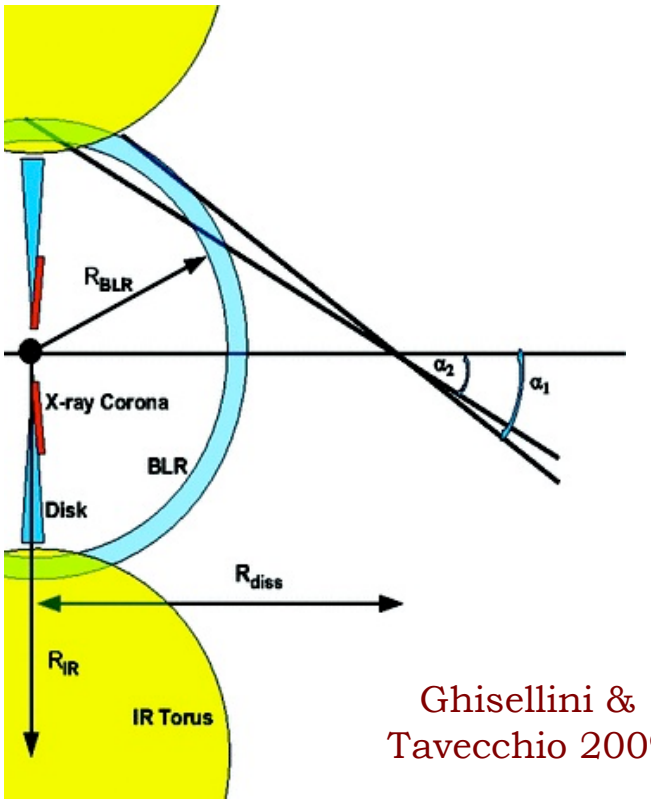

Ghisellini & Tavecchio 2009

Heavy Jets

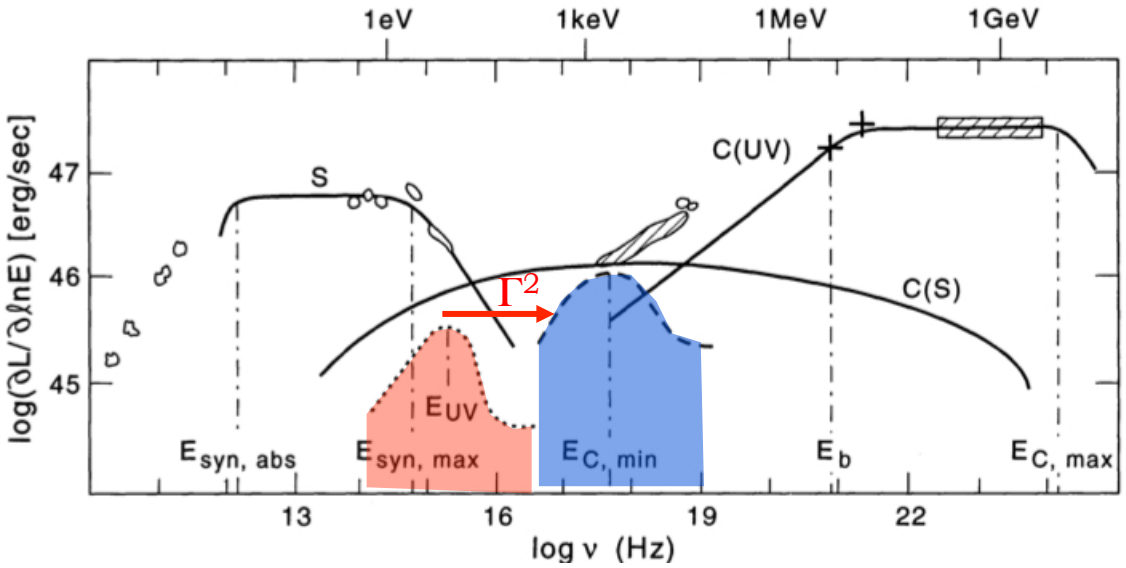

Lack of bulk-Compton features in soft-X-ray spectra of blazars indicates that there are not enough cold electrons to carry bulk of the jet kinetic power. This indicates a dynamical role of (cold) protons (Begelman & Sikora 1987, Sikora et al. 1997, Sikora & Madejski 2000, Celotti et al. 2007, Celotti & Ghisellini 2008, Kataoka et al. 2008)

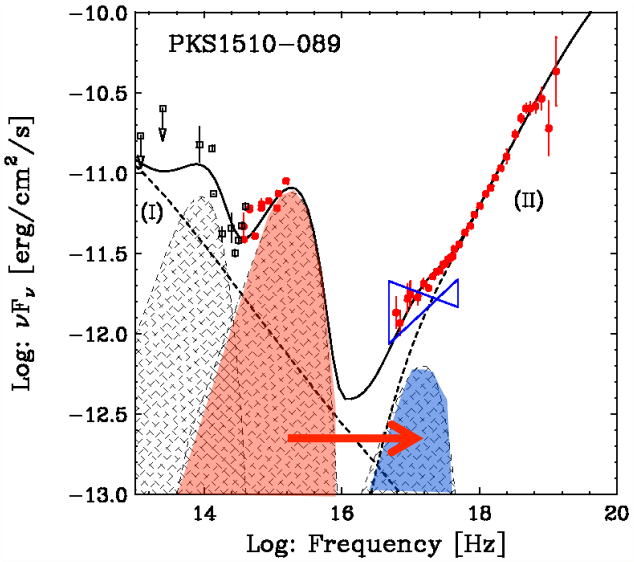

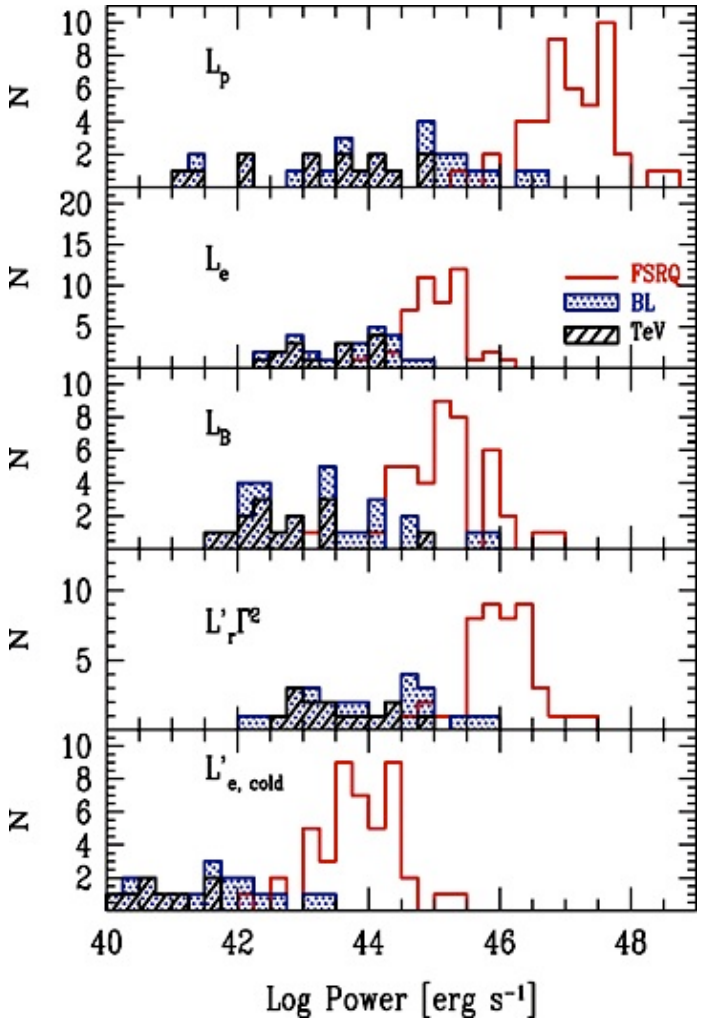

GeV Spectral Breaks

Fermi/LAT discovered that gamma-ray spectra of luminous FSRQs are typically of a broken power-law form, with spectral breaks located around a few GeV (e.g., PKS 1222+216).

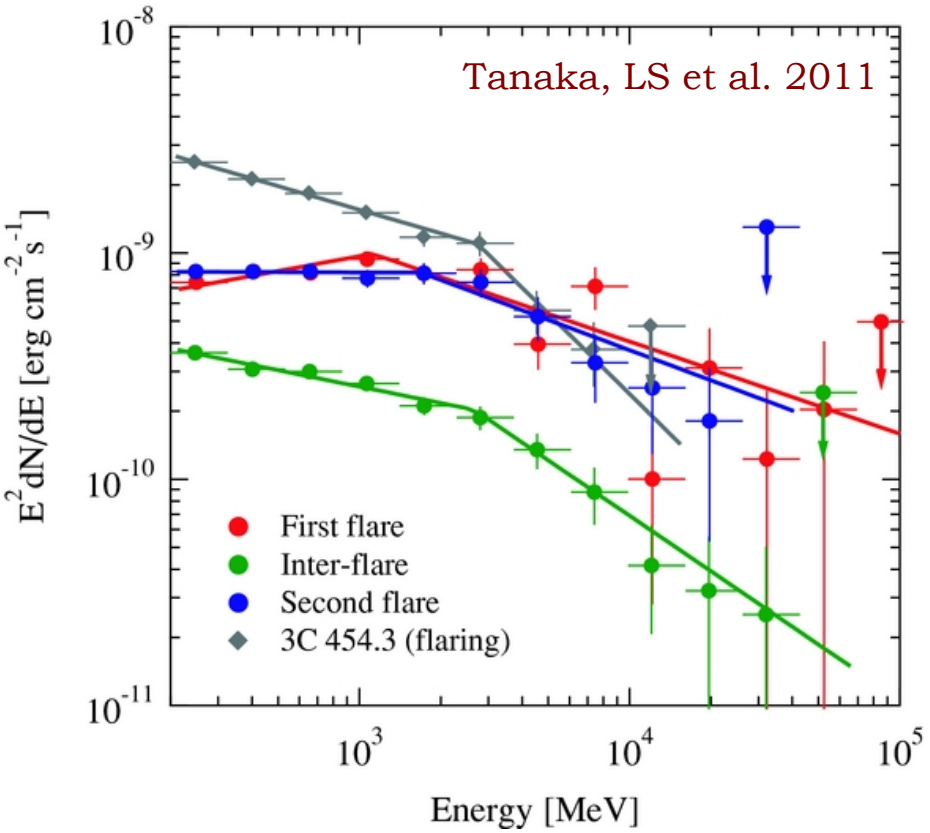

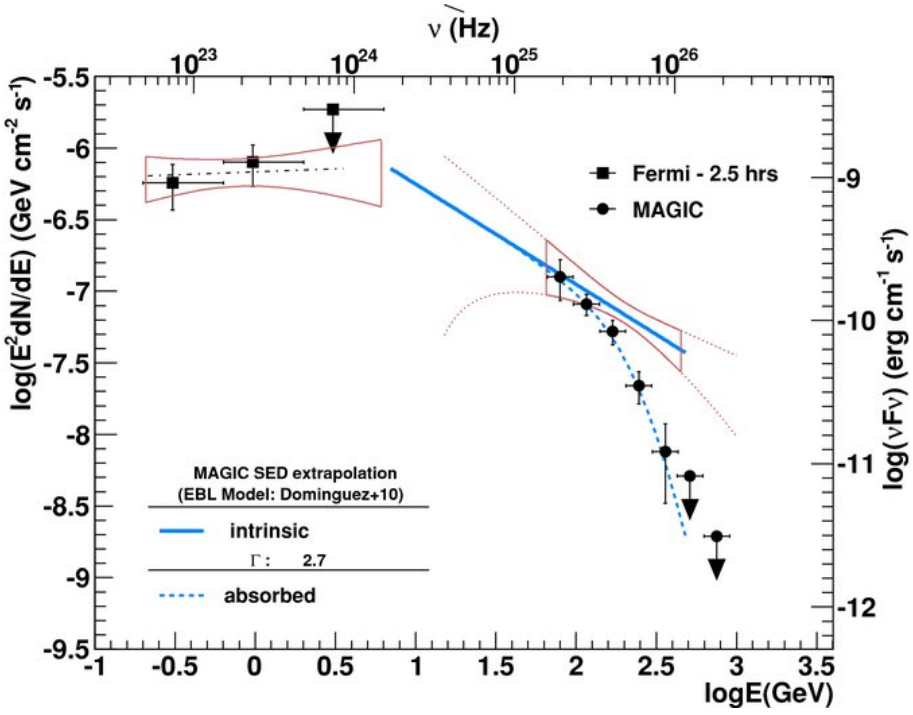

Aleksic et al. 2011

The mosr recent studies reveal variety of particle spectra resulting from 1st-order (diffusive) Fermi acceleration at relativistic shocks, depending on the magnetic field configuration (subluminal or superluminal shocks), and turbulence spectrum (e.g., Niemiec & Ostrowski 2006, Lemoine et al 2006, Spikovsky et al. 2010). **There is no universal spectral shape of shock-accelerated particles!**

Problems!

Hayashida et al. 2012

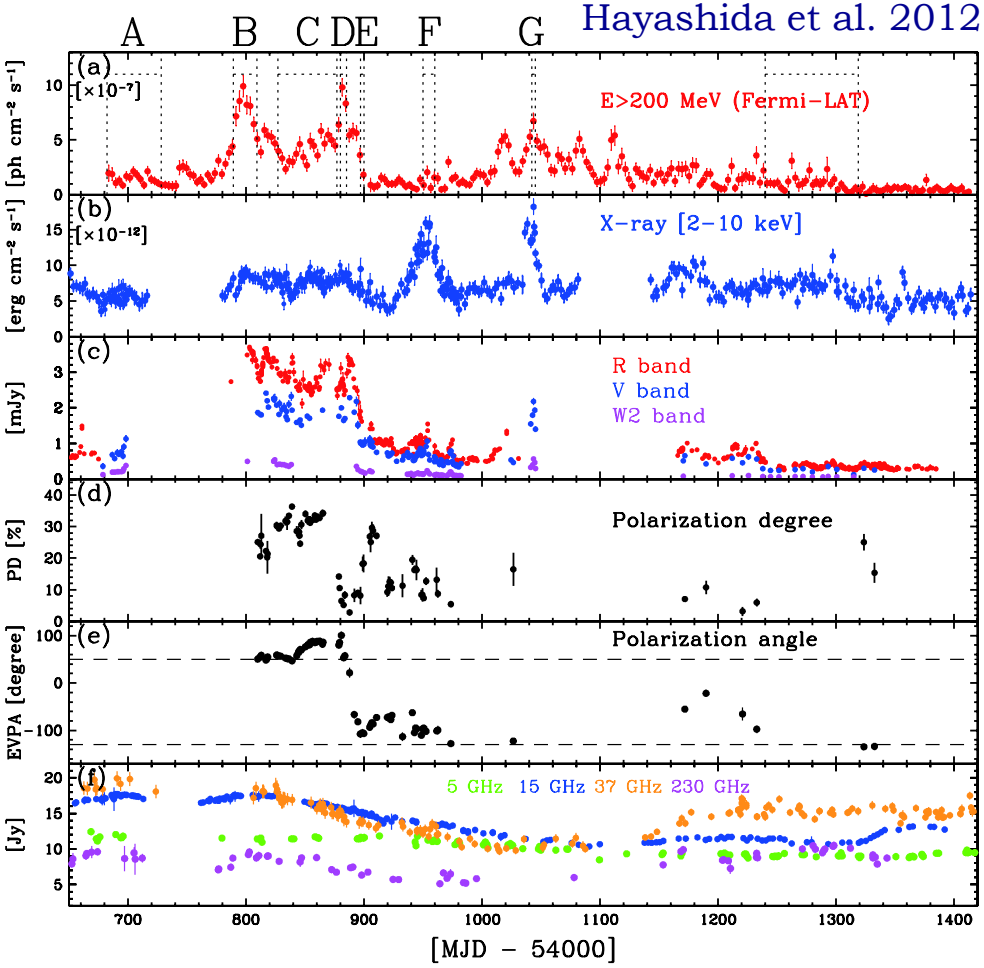

Boettcher et al. 2009

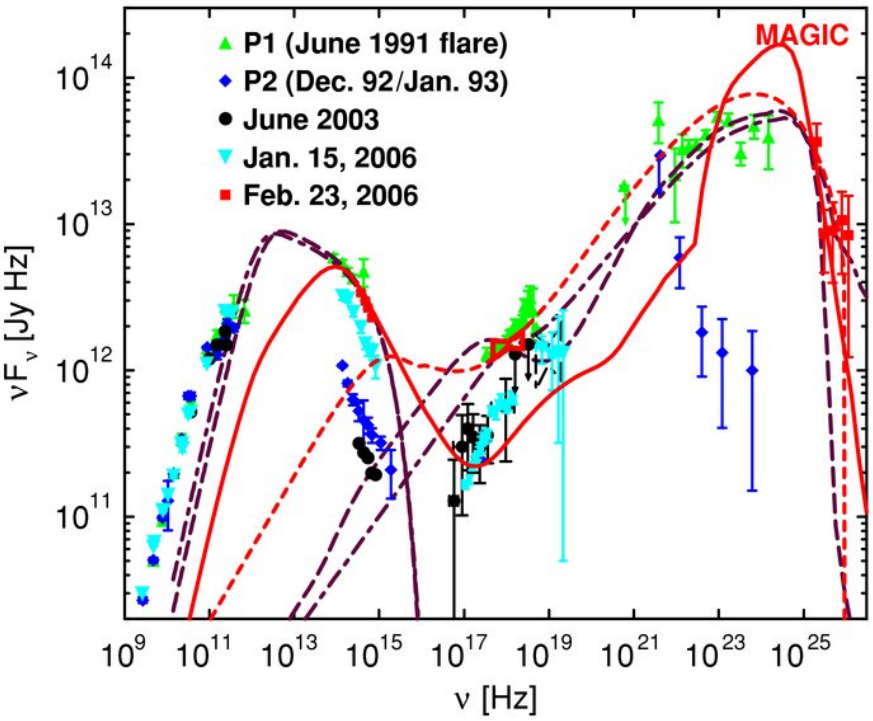

No GeV/X-ray correlations, no obvious GeV/radio correlations,
surprising and unexpected very fast TeV flares…

Cosmology

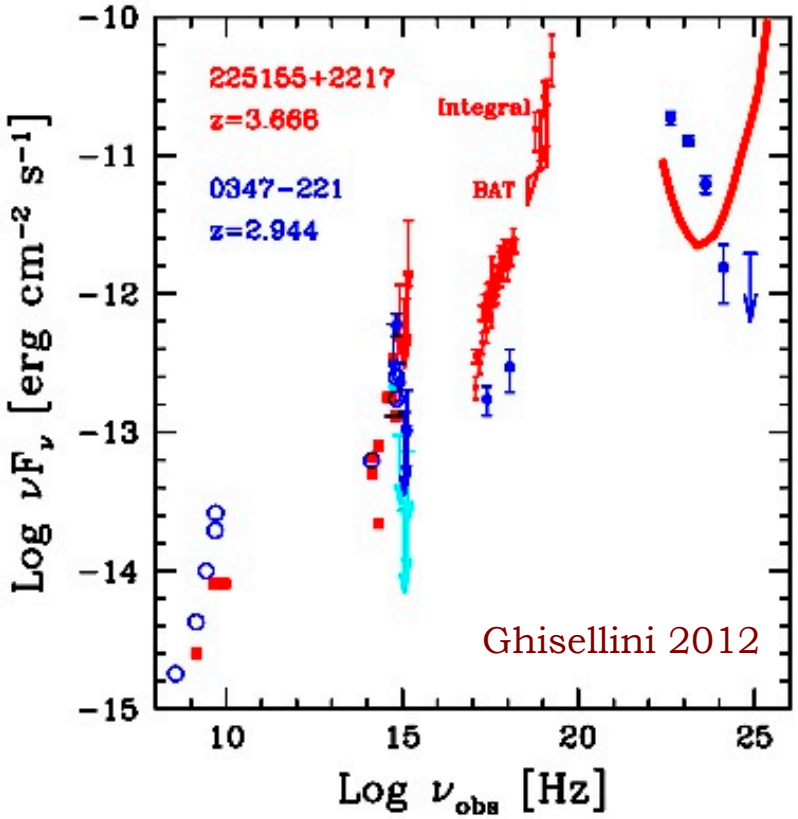

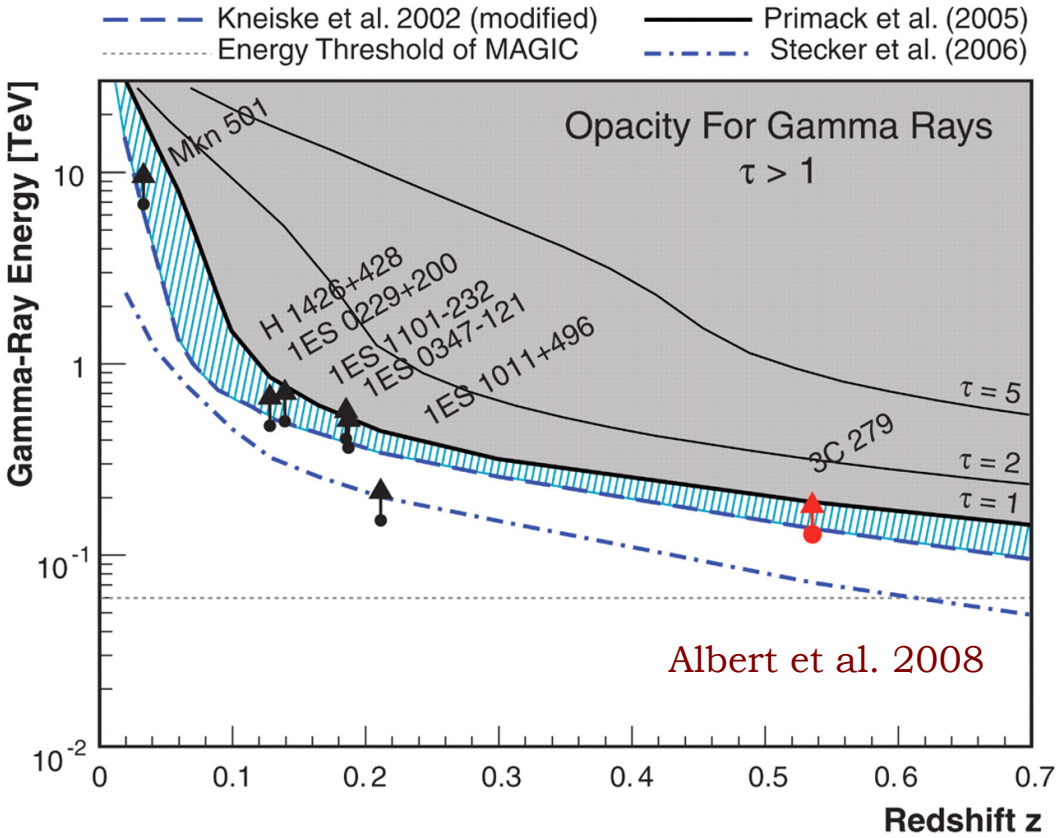

TeV detections of distant (z>0.2) FSRQs are interesting in the context of constraining the cosmological evolution of EBL.

Deep hard X-ray observations may be the most efficient way of studying SMBHs and relativistic jets in high-redshift (z>2) blazars of the FSRQ type.

Radio Galaxies

Radio galaxies are believed to constitute the parent population of blazar sources. Unlike in blazar sources, the observed X-ray emission of radio galaxies is significantly contributed, or sometimes even entirely dominated by the emission of the accretion disks and disk coronae. This constitutes an opportunity to investigate the jet-disk coupling, and hence the jet launching processes, by means of joint X-ray and gamma-ray observations.

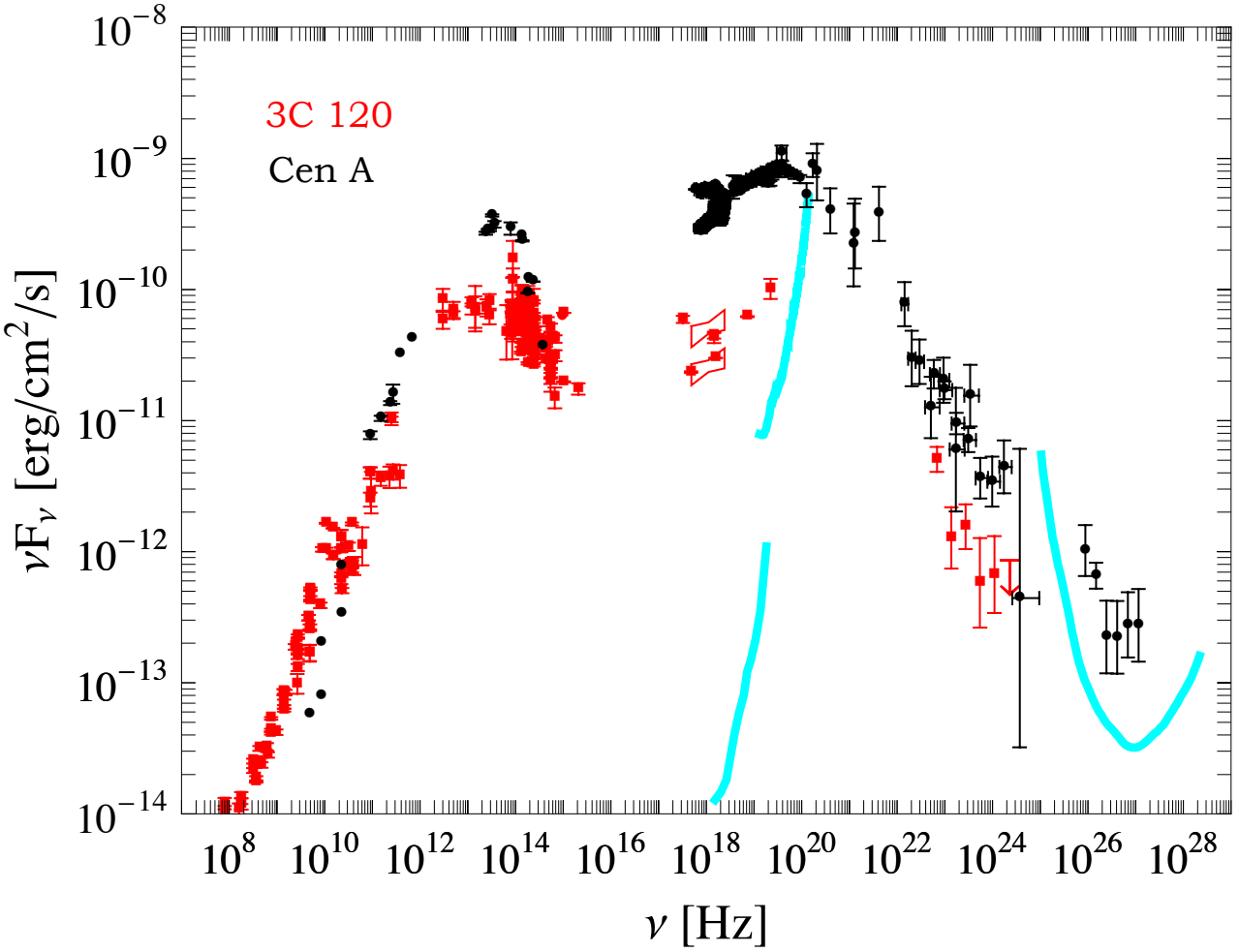

Growing Population

Table 1. *Fermi*-LAT Non-Blazar AGN & Galaxies

name	R.A. J2000	Dec. J2000	z	class	LAT	Γ_γ	$F_{1-100\,\mathrm{GeV}}$ $[10^{-9}/\mathrm{cm}^2/\mathrm{s}]$	var.	TeV	comments
(1)	(2)	(3)	(4)	(5)	(6)	(7)	(8)	(9)	(10)	(11)
PKS 0625−35	06h27m06.7s	−35d29m15s	0.055	FR I/BL Lac	1FGL, 2FGL	1.93±0.09	1.50±0.18	—	—	cD in Abell 3392
IC 310	03h16m43.0s	+41d19m30s	0.019	FR I/BL Lac	2FGL	2.10±0.19	0.88±0.23	—	Y/V	in Perseus
3C 78	03h08m26.2s	+04d06m39s	0.029	FR I	1FGL	1.95±0.14	0.52	?	—	
Per A	03h19m48.1s	+41d30m42s	0.018	FR I	1FGL, 2FGL	2.00±0.02	18.8±0.53	V	Y/V	CSO; cD in Perseus
M 87	12h30m49.4s	+12d23m28s	16 Mpc	FR I	1FGL, 2FGL	2.17±0.07	1.73±0.18	—	Y/V	cD in Virgo
Cen A	13h25m27.6s	−43d01m09s	3.7 Mpc	FR I	1FGL, 2FGL	2.76±0.05	3.03±0.24	—	Y	GeV lobes
NGC 6251	16h32m32.0s	+82d32m16s	0.025	FR I	1FGL, 2FGL	2.2±0.07	1.15±0.14	V?	—	GRG; GeV lobes?
Fornax A	03h22m41.7s	−37d12m30s	19 Mpc	FR I/FR II	2FGL	2.16±0.15	0.53±0.12	—	—	cD in Fornax; GeV lobes?
Cen B	13h46m49.0s	−60d24m29s	0.013	FR I/FR II	2FGL	2.33±0.12	1.86±0.34	—	—	GeV lobes?
PKS 0943−76	09h43m23.9s	−76d20m11s	0.270	FR II	1FGL, 2FGL	2.44±0.14	0.71±0.16	—	—	
3C 120	04h33m11.1s	+05d21m16s	0.033	FR II, BLRG	(MAGN, K11)	3.00±0.30	0.4	V	UL	superlum. jet
3C 111	04h18m21.3s	+38d01m36s	0.049	FR II, BLRG	1FGL	2.70±0.20	0.70	V	UL	superlum. jet
3C 207	08h40m47.6s	+13d12m24s	0.681	FR II/SSRQ	1FGL, 2FGL	2.36±0.11	0.76±0.14	V?	—	
3C 380	18h29m31.8s	+48d44m46s	0.692	FR II/SSRQ	1FGL, 2FGL	2.34±0.07	1.37±0.16	V?	—	CSS
4C 55.17	09h57m38.2s	+55d22m58s	0.896	RQ	1FGL, 2FGL	1.83±0.03	11.2±0.38	—	—	CSO
PKS 2004−447	20h07m55.2s	−44d34m44s	0.240	NLSy	1FGL, 2FGL	2.47±0.12	0.66±0.14	—	—	CSS
1502+036	15h05m06.5s	+03d26m31s	0.409	NLSy	1FGL, 2FGL	2.51±0.07	1.37±0.17	—	—	
0323+342	03h24m41.1s	+34d10m46s	0.061	NLSy	1FGL, 2FGL	2.69±0.21	0.54	V	—	
PMN J0948+0022	09h48m57.3s	+00d22m26s	0.585	NLSy	1FGL, 2FGL	2.26±0.08	2.17±0.22	V	—	
ESO 323−G077	13h06m26.1s	−40d24m52s	0.015	Sy 1	(1FGL), 2FGL	2.33±0.13	0.67±0.15	—	—	
NGC 6814	9h42m40.6s	−10d19m25s	22 Mpc	Sy 1.5	2FGL	2.54±0.14	0.68±0.16	—	—	
NGC 1068	02h42m40.7s	−00d00m48s	17 Mpc	Sy 2	1FGL, 2FGL	2.15±0.17	0.51±0.11	—	UL	γ-rays due to ISM
NGC 4945	13h05m27.5s	−49d28m06s	3.7 Mpc	Sy 2	1FGL, 2FGL	2.10±0.15	0.75±0.17	—	—	γ-rays due to ISM
M 82	09h55m52.7s	+69d40m46s	3.4 Mpc	G	1FGL, 2FGL	2.28±0.09	1.02±0.13	—	Y	γ-rays due to ISM
NGC 253	00h47m33.1s	−25d17m18s	2.5 Mpc	G	1FGL, 2FGL	2.31±0.13	0.62±0.12	—	Y	γ-rays due to ISM

Not including Local Group Galaxies (SML, LMC, M31, MW)

Low-Power, Nearby

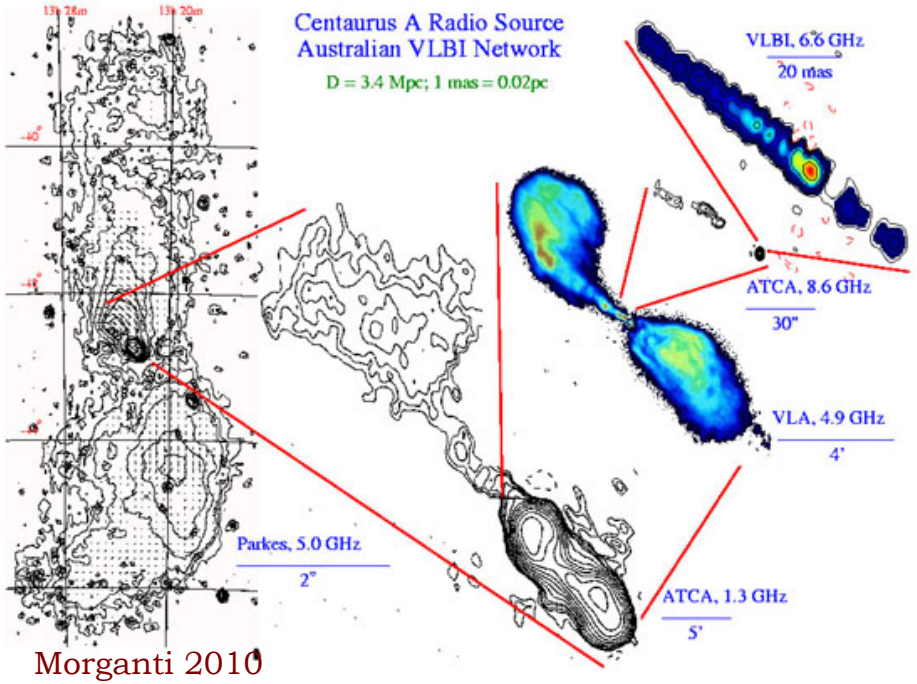

Morganti 2010

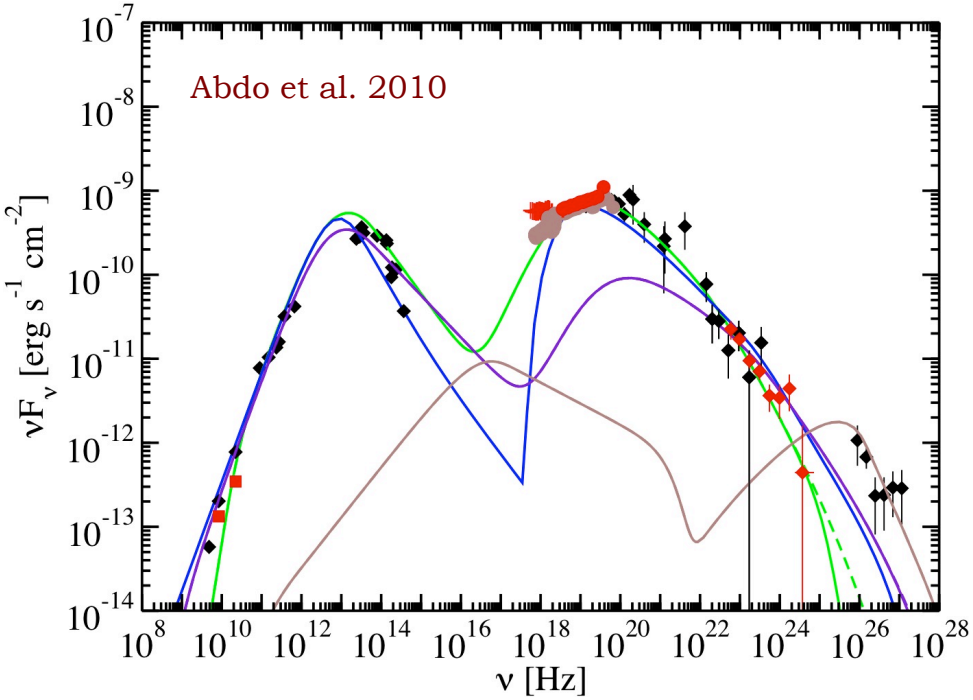

Centaurus A:
giant low-power (FR I) radio galaxy, only 3.7 Mpc away, detected by all the instruments onboard CGRO, by Fermi/LAT, and HESS in the 100 keV - 10 TeV range.

Giant Lobes

Fermi/LAT

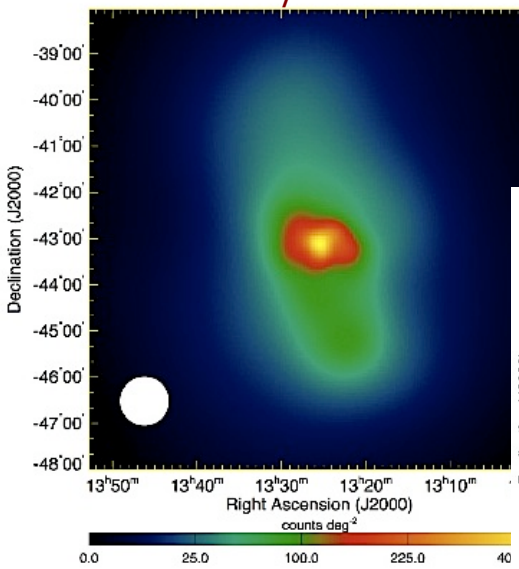

WMAP

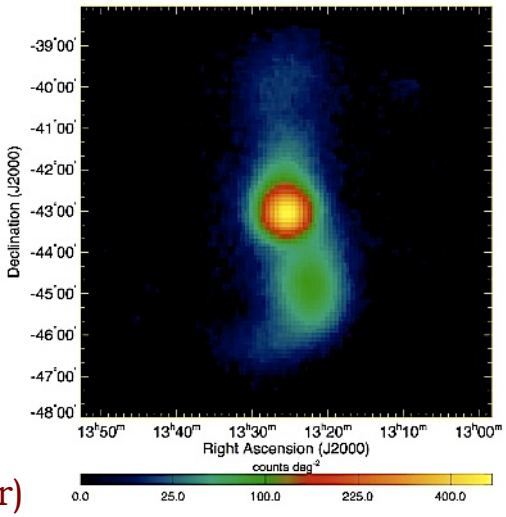

Abdo et al. 2010
(CAs: Cheung, LS,
Fukazawa, & Knodlseder)

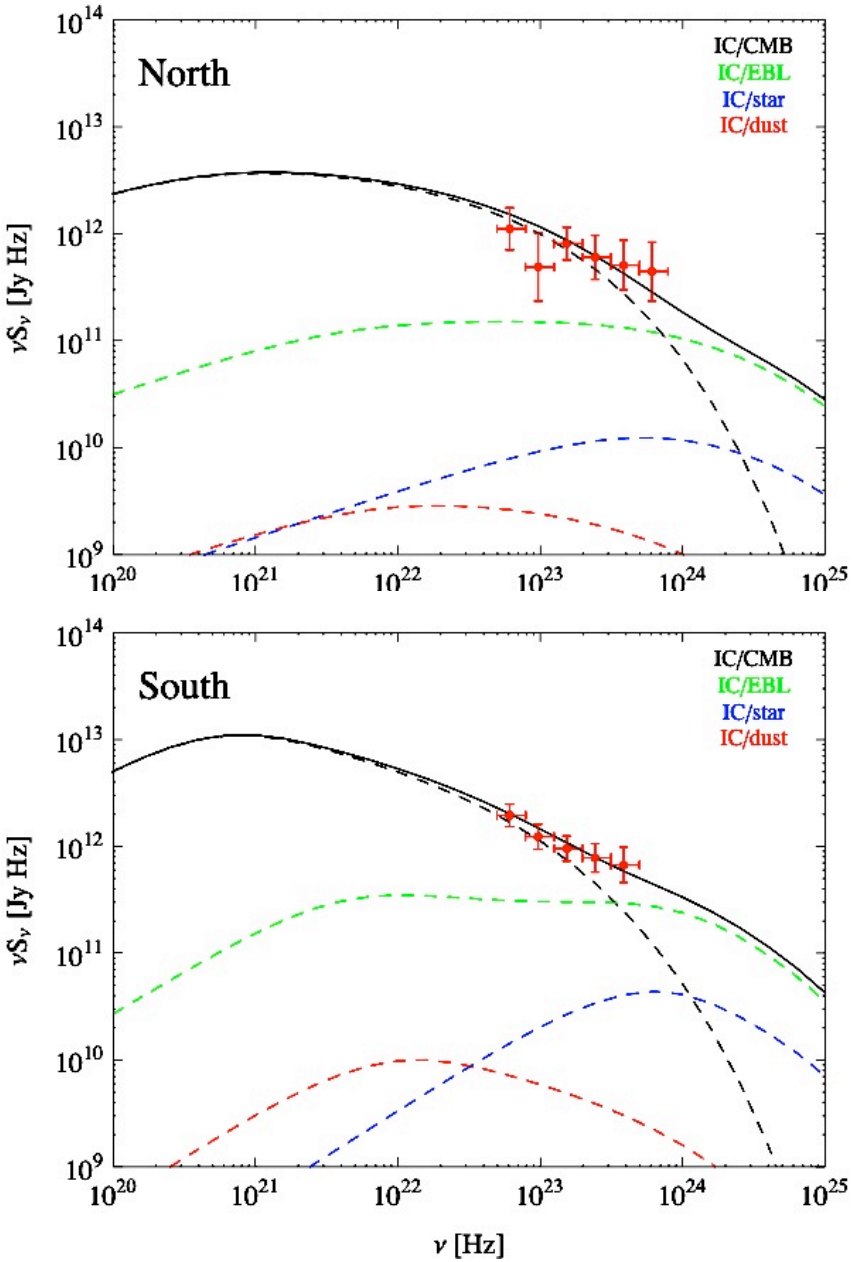

Fermi/LAT (similarly as WMAP) resolved giant lobes of Centaurus A radio galaxy (~8 deg on the sky, ~1Mpc physical size).

X-ray and TeV mapping of the giant halo awaits future observations.

Jet/Disk Connection

The long-term monitoring of 3C 120 at X-ray and radio frequencies suggested that the dips in the X-ray emission are followed by ejections of bright superluminal knots along the radio outflow. The proposed interpretation involved X-ray dips due to the disappearance of the inner parts of the accretion disk leading to the ejection of the excess matter along the jet axis, analogous to what is observed in the Galactic jet sources.

The possibility that the related phenomenon may be also observed at gamma-rays, with the gamma-ray flares following the dips in the accretion-related X-ray emission, awaits the operation of CTA and ASTRO-H.

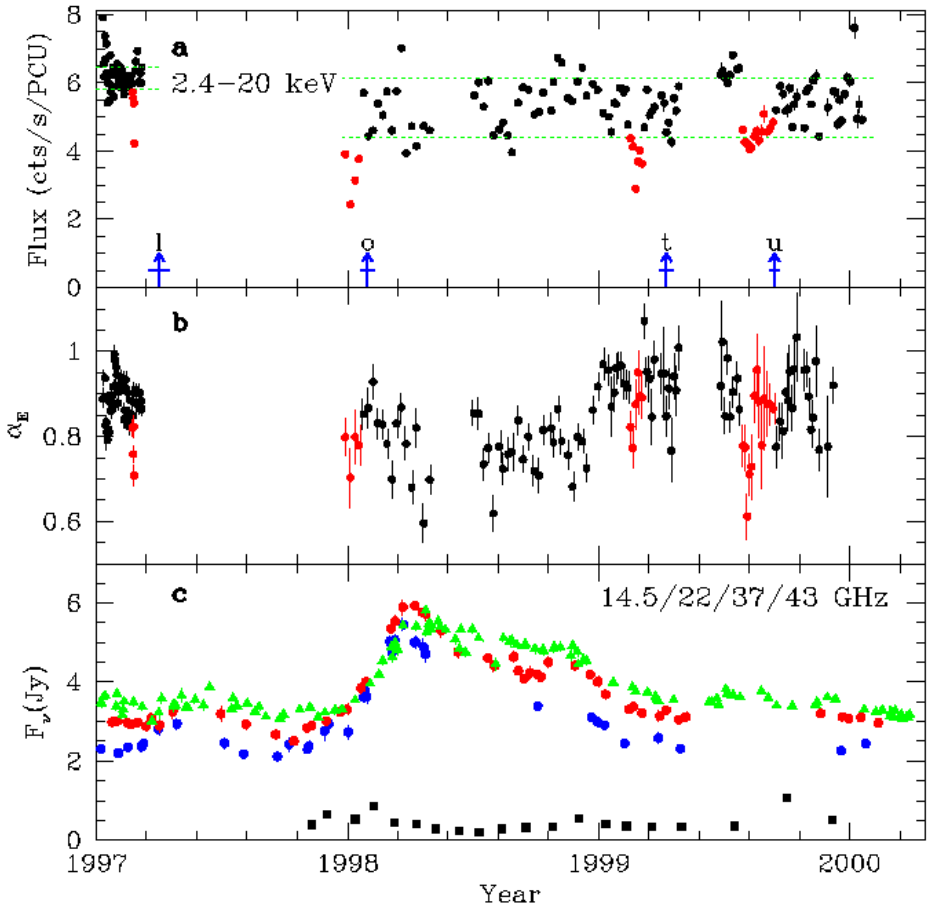

Marscher et al. 2002

Seyfert Galaxies

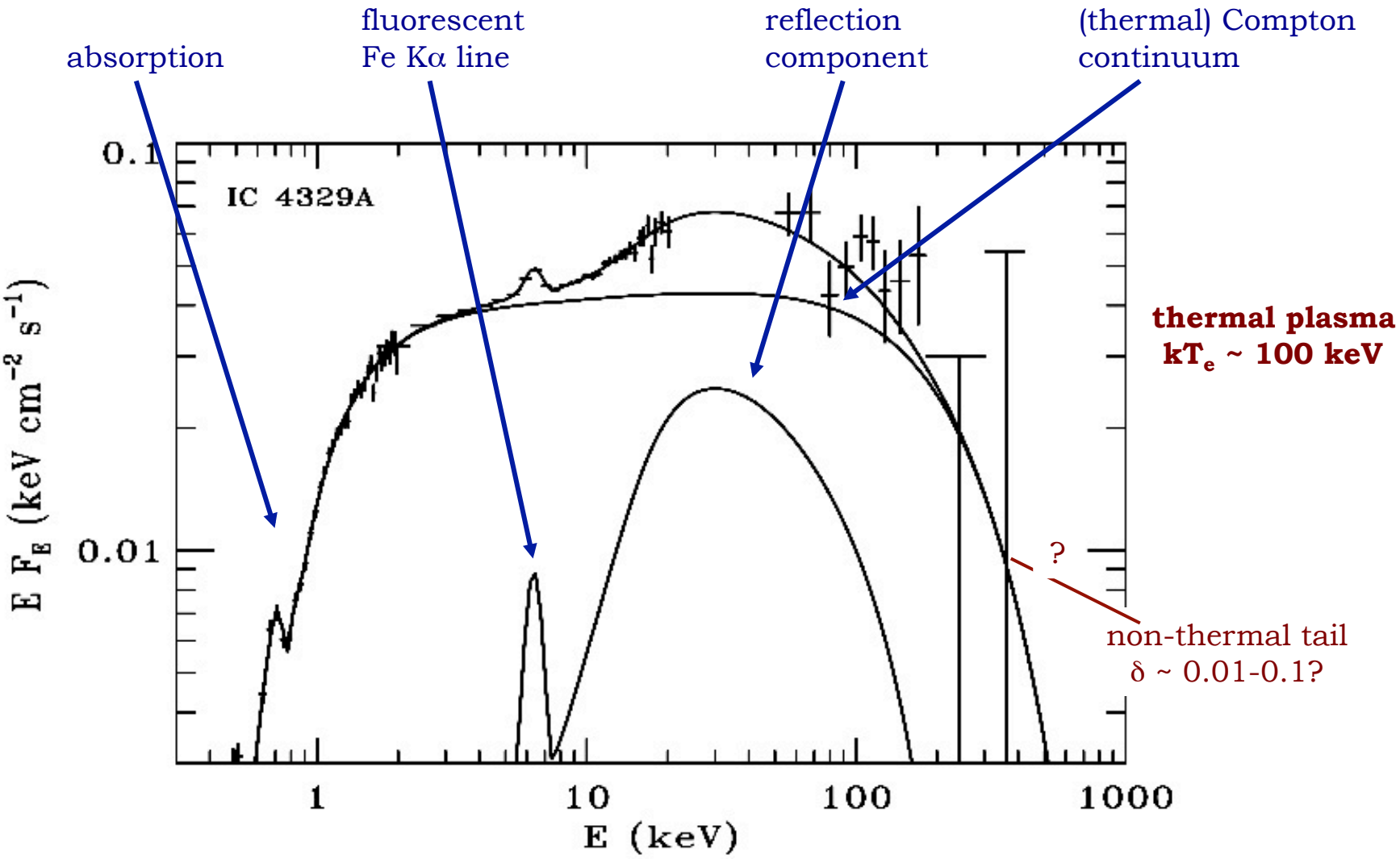

High energy (X-ray/soft γ-ray) emission of Seyfert galaxies is widely believed to be dominated by the accreting matter (e.g., Zdziarski 1999, Poutanen 1998)

Strictly Thermal?

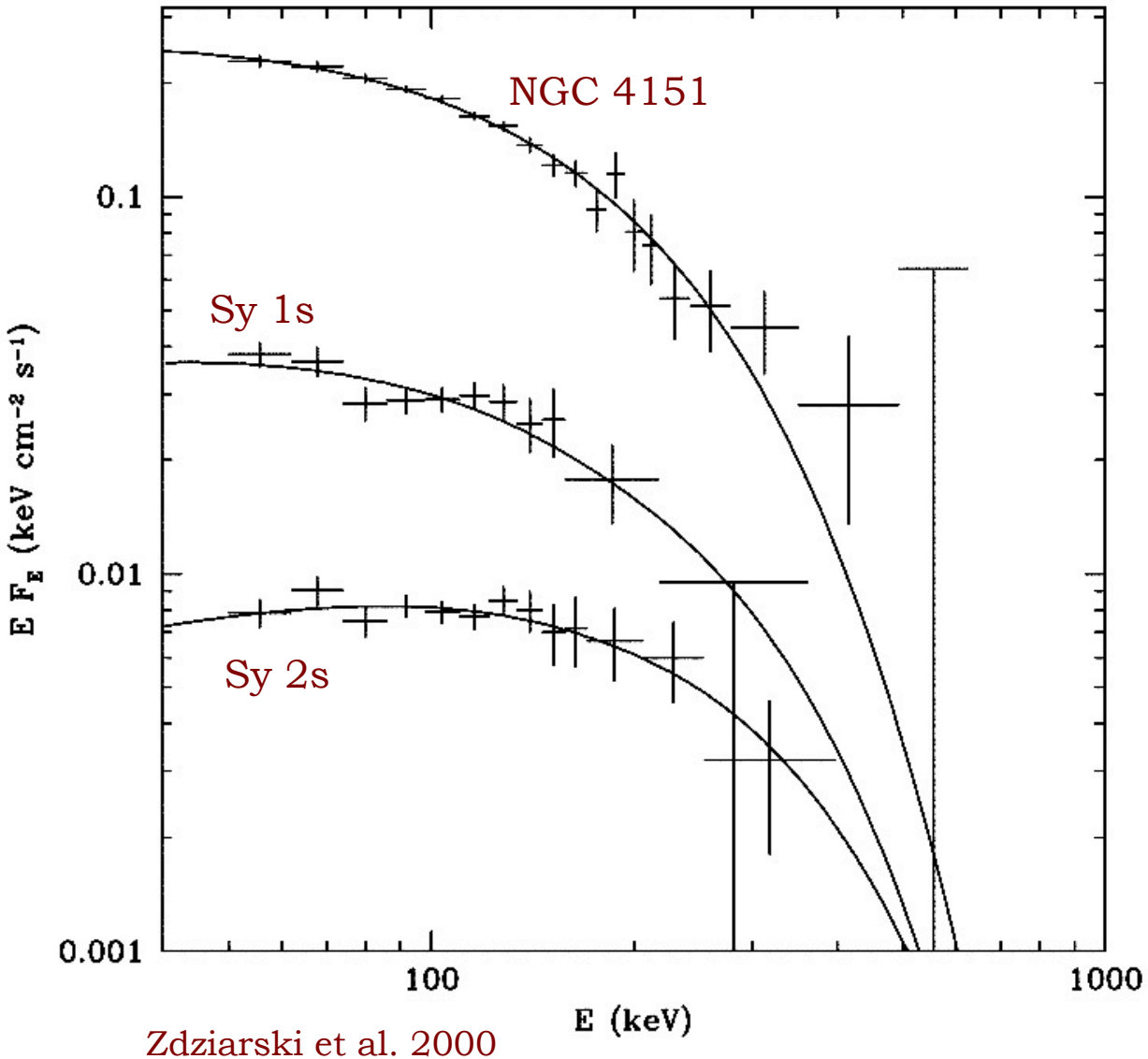

Zdziarski et al. 2000

Non-thermal models for X-ray/soft γamma-ray spectra of Seyferts were widely discussed in the 80s/90s. However, OSSE observations suggesting cut-offs in the spectra of Seyferts around 100 keV implied that thermal models are more likely. Still, OSSE sensitivity was rather limited, and the number of OSSE-detected Seyferts was rather low.

$\delta < 0.1$ on average.

Non-thermal Coronae

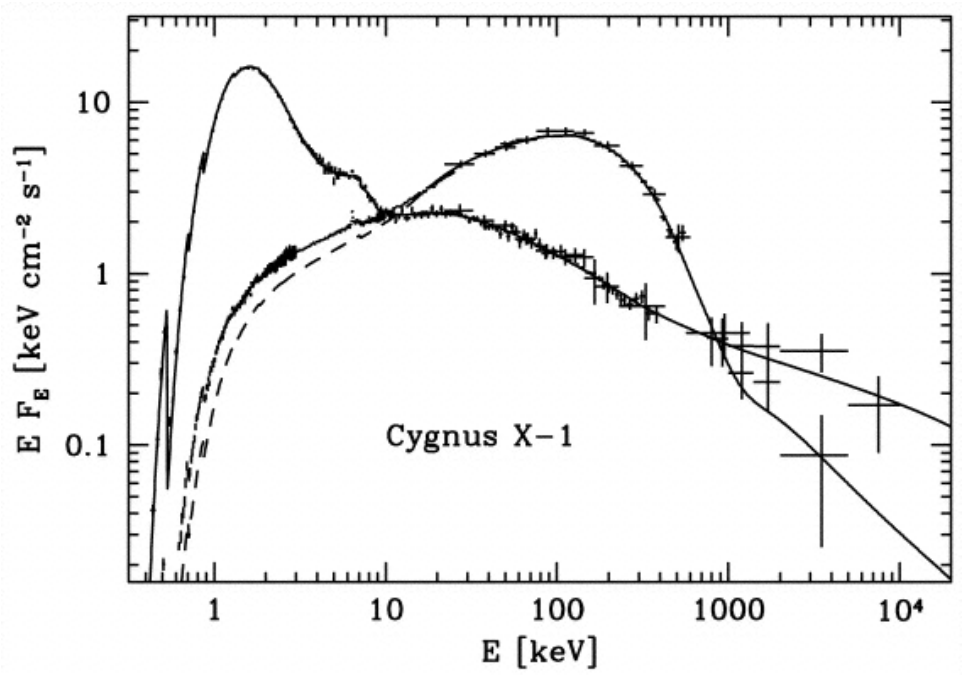

Galactic source Cygnus X-1 detected at 1-10 MeV photon energies (particularly in its "low hard" state), and also (possibly?) at TeV energies.

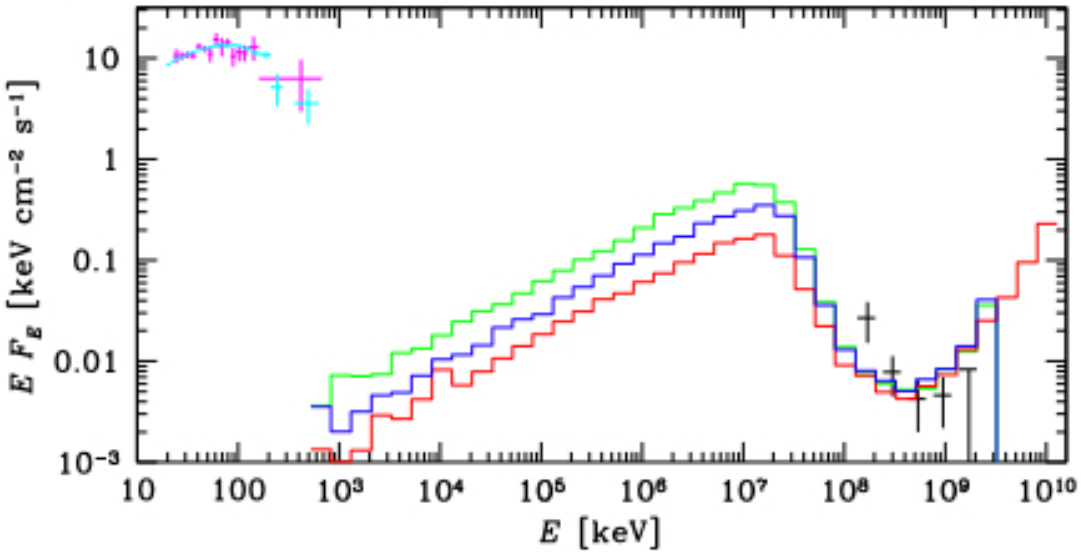

TeV emission of Cygnus X-1 modeled as produced by non-thermal particles accelerated by turbulence and reconnection within the accretion flow (disk coronae) and heavily absorbed by the surrounding photon fields (leading to the formation of a cascade emission; Zdziarski et al. 2009).

What If ... ?

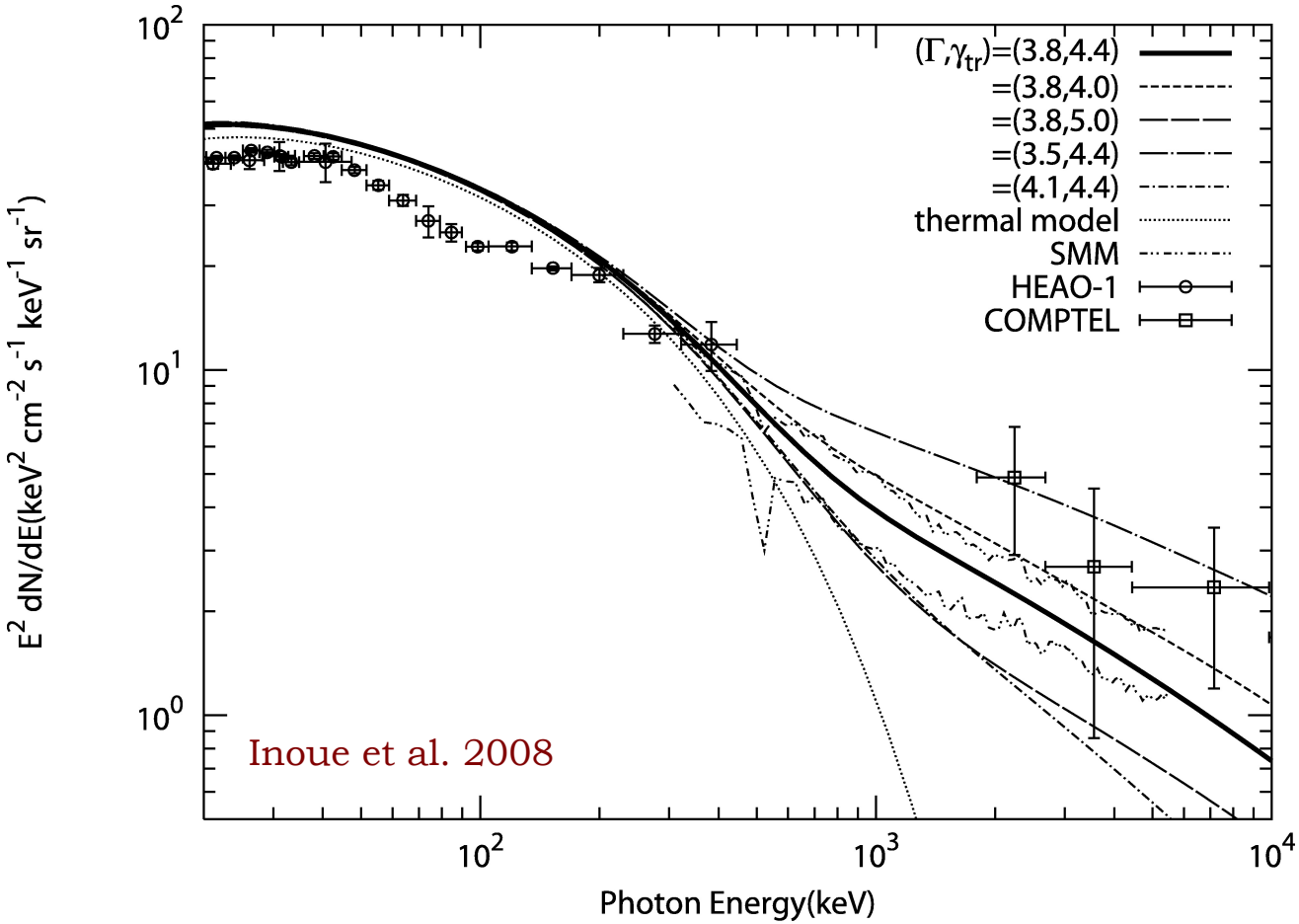

Extragalactic MeV background may be explained by radio-quiet (Seyfert-like) AGN, assuming a presence of non-thermal electrons in hot and highly magnetized coronae of their accretion disks (acceleration to ultrarelativistic energies driven by magnetic reconnection), at the level $\delta \sim 0.01$-0.1.

Gamma-ray Quiet?

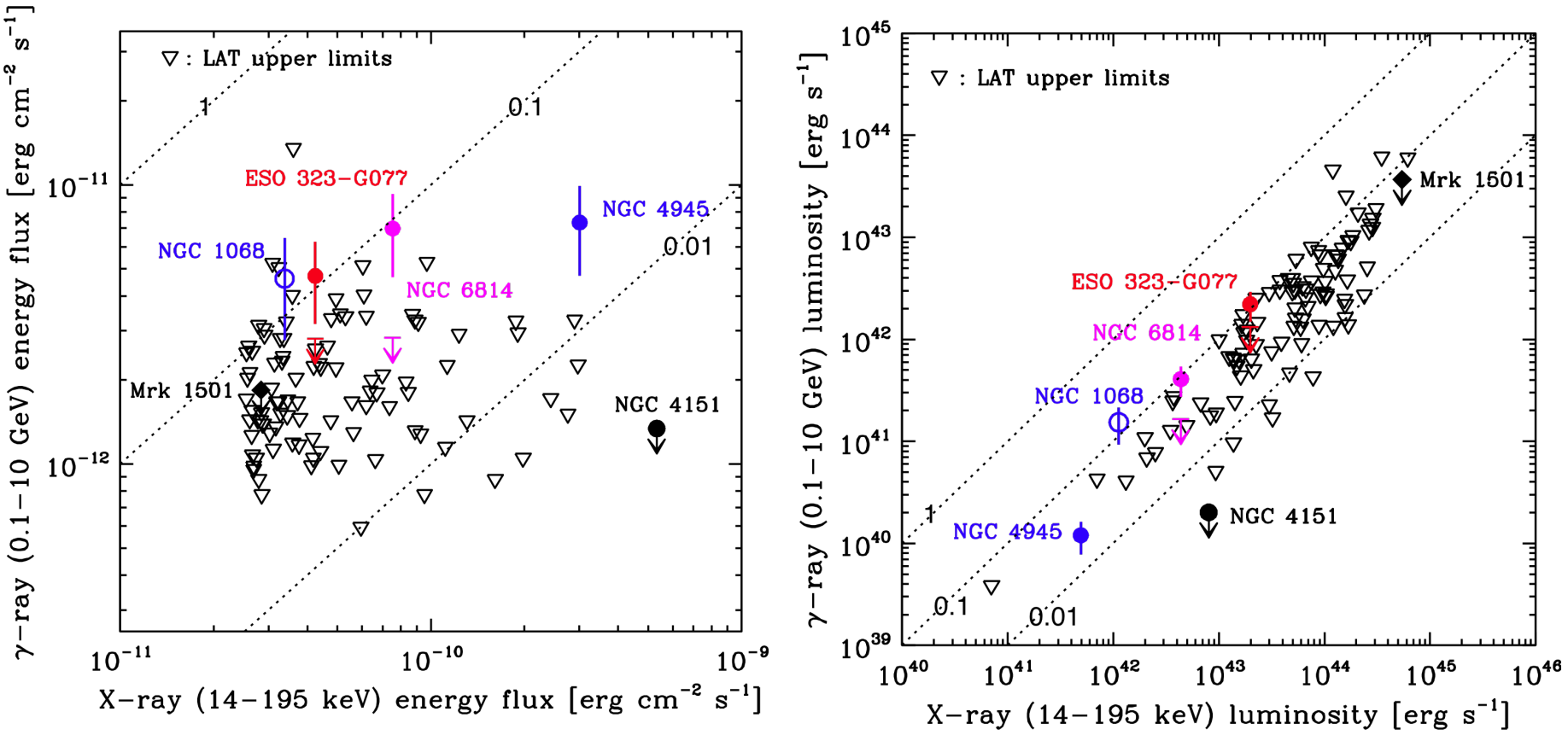

No statistically significant gamma-ray excess coincident with any hard X-ray brightest Seyfert galaxy, with possible exceptions of ESO 323–G077 and NGC 6814. The Fermi–LAT upper limits probe the ratio of gamma-ray to X-ray luminosities < 10%, and even < 1% in some cases
(Ackermann et al. 2012; CAs: Hayashida, LS, Madejski, & Bechtol).

Clusters of Galaxies

Merging processes leading to the formation of clusters of galaxies release huge amounts of gravitational energy ($\geq 10^{64}$ erg) on timescales of the order of ~Gyr.
While much of this energy is contained in thermal plasma with temperatures 10 keV emitting X-ray photons via the bremsstrahlung process, part of it may be channelled to accelerate a small fraction of particles from the thermal pool to ultrarelativistic energies (e.g., on giant accretion shocks), and to form in this way an energetically relevant hadronic CR population within the ICM.

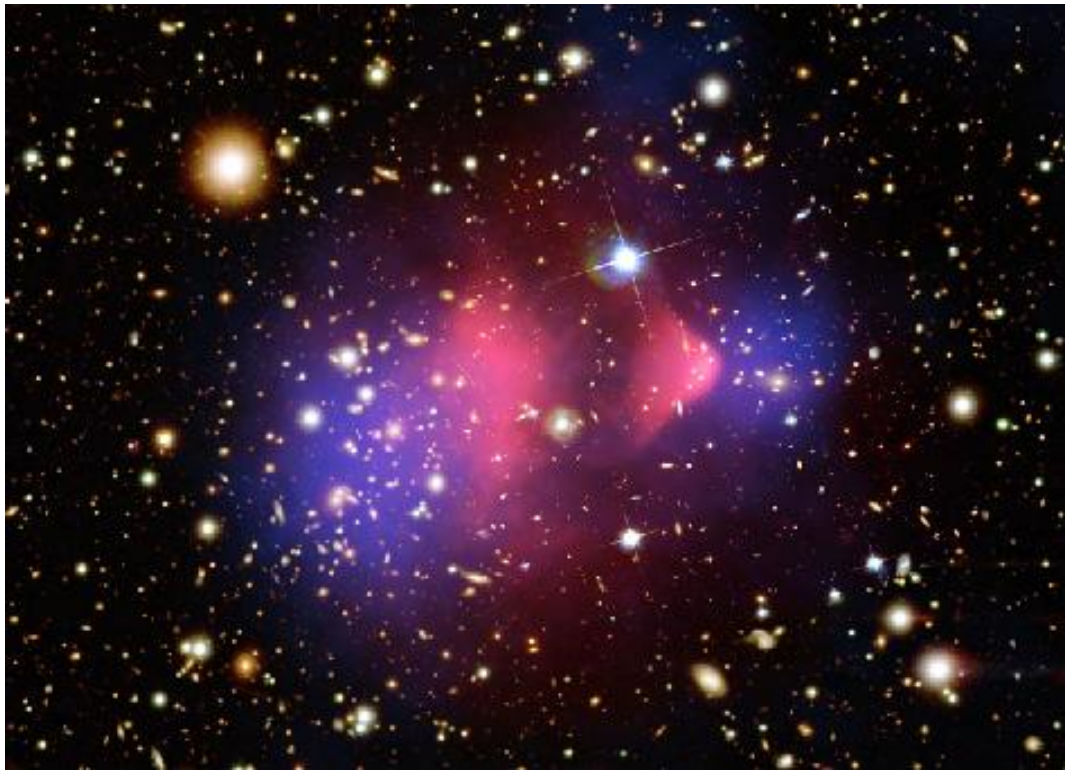

Bullet cluster

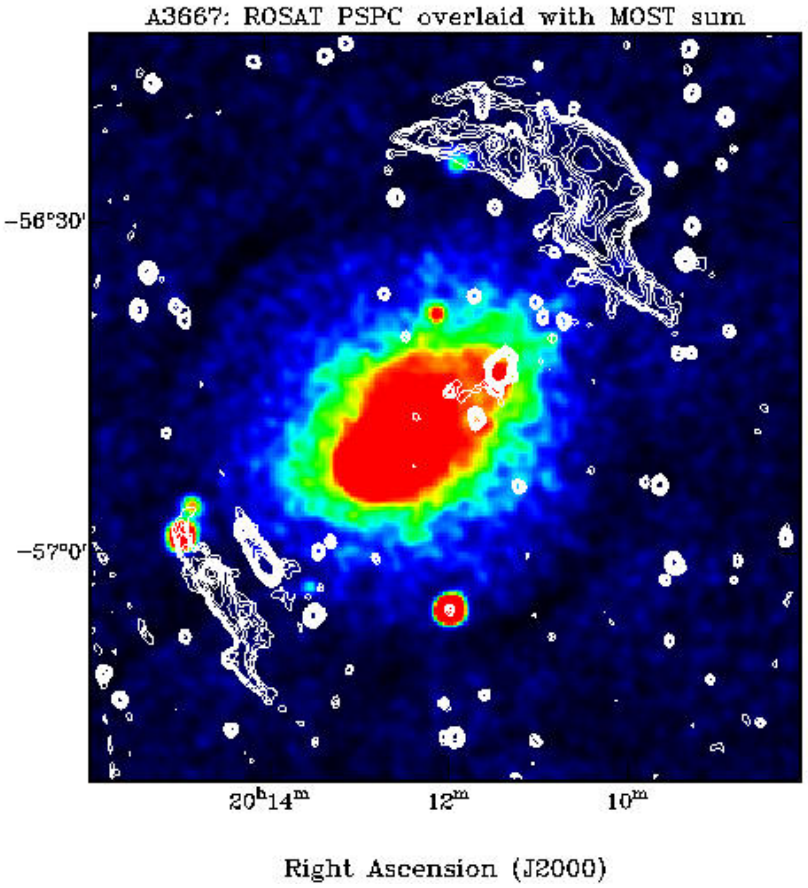

Giant Radio Halos

Non-thermal activity in the ICM manifests clearly in the phenomenon of giant (~Mpc-scale) radio halos. These are roughly spherical and low-surface brightness structures centered at the position of the peaks in galaxy distributions, which are found in about 10% of the systems.

Are these due to the electrons formed as secondaries from hadronic CR interactions, electrons produced via DM annihilation/decay processes, or electrons accelerated as primary CRs directly from the thermal pool of the ICM by the magnetic turbulence (stochastic processes)?

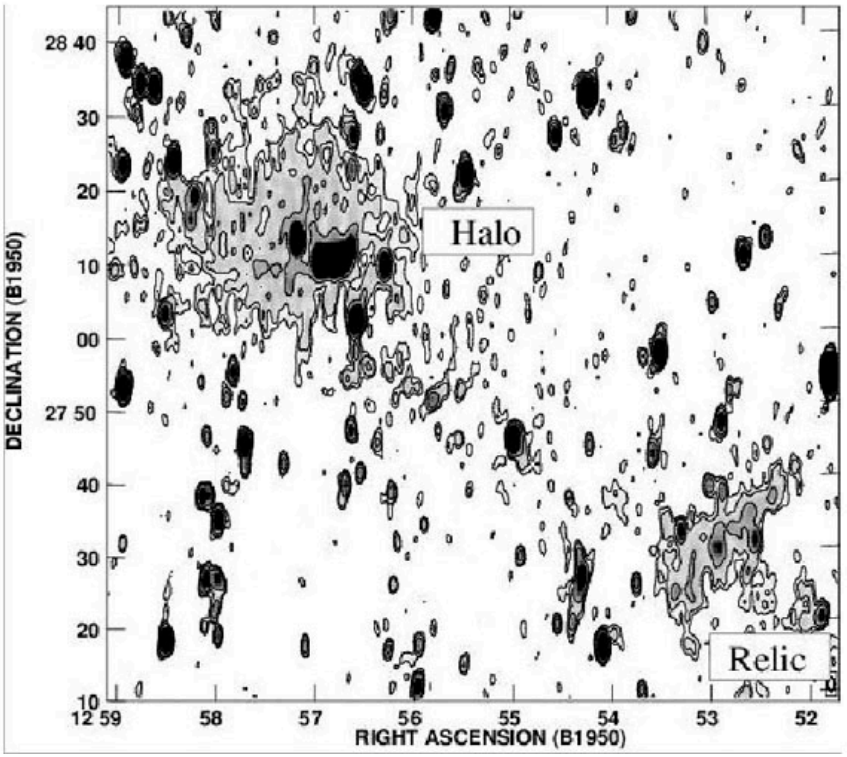

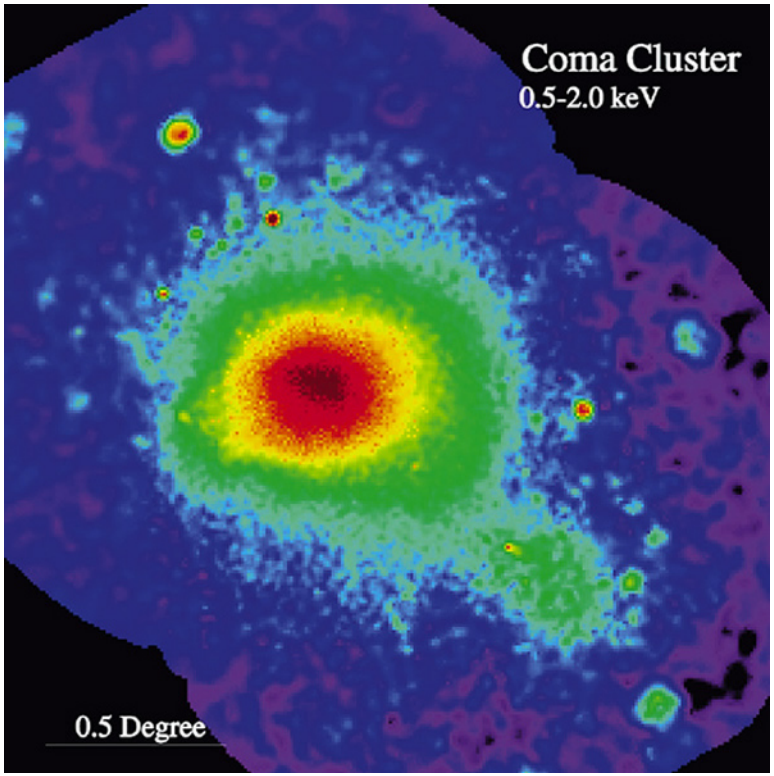

Coma cluster

DM, Shocks, Turbulence…

A variety of choices regarding the candidates for the DM particles, not fully constrained particle acceleration mechanisms, and hardly known turbulence conditions within the ICM due to the insufficient knowledge regarding the kinematics of the cluster gas and the structure of the cluster magnetic fields, all affect the model predictions regarding the spatial distribution and the energy spectra of the non-thermal emission of clusters of galaxies.

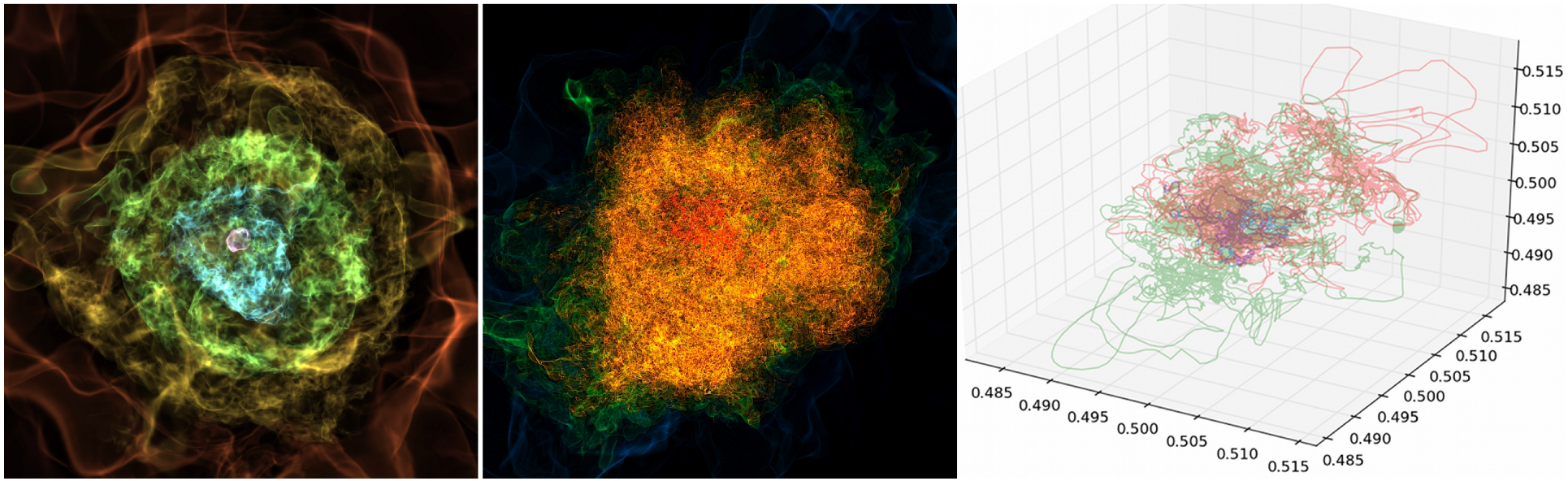

Xu et al. 2009: Isocontours of baryon density (left), magnetic field strength (middle), and magnetic field lines at $z = 0$. The field of view is 6 Mpc. The color ranges are 1e-10 (blue) to 2e-6 (red) G for magnetic fields.

Coma Cluster

Swift & Suzaku hard X-ray upper limit: Wik et al. 2011.
Fermi/LAT upper limit: Ackermann et al. 2011 (point source, King profile, 2D Gaussian 0.8deg).
HESS upper limits: Aharonian et al. 2009 (source region radius 0, 0.2 and 0.4deg).
Solid curves: turbulence/leptonic model for cluster magnetic field 2, 5 μG (Brunetti & Lazarian 2011).
Dashed curves: DM-induced emission for the neutralino mass of 60 GeV (Colafrancesco et al. 2011).
Thick line: shock/hadronic model (Pfrommer 2008, Pinzke et al. 2010).

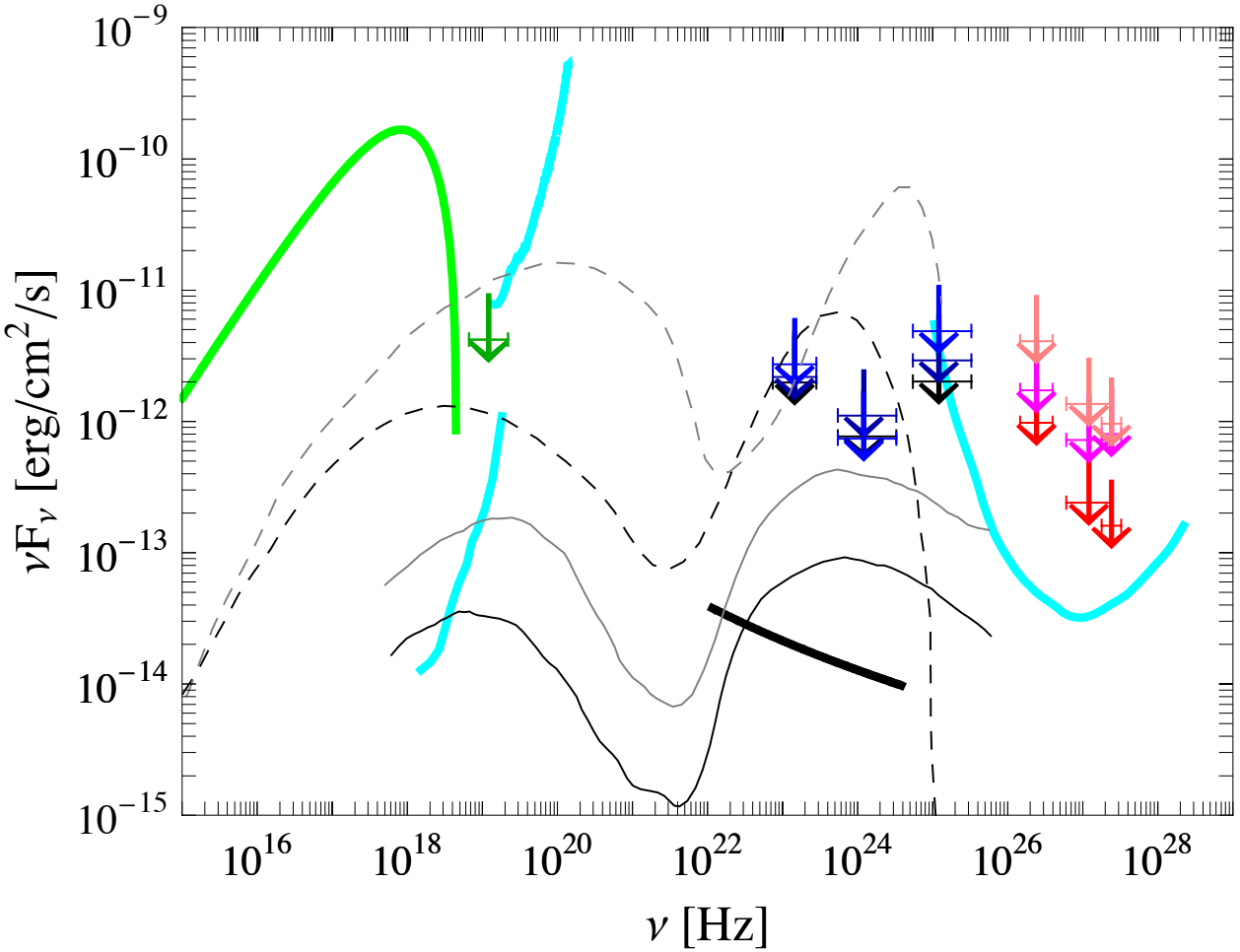

ICM Spectroscopy

Detailed insight into the kinematics of the ICM, and hence into the various energy dissipation processes involved, thanks to spectrometric observations probing bulk plasma velocities and/or turbulence at a resolution corresponding to a speed of a few times 100km/s, together with an arcmin imaging system in the hard X-ray band with a sensitivity of orders of magnitude better than previous missions

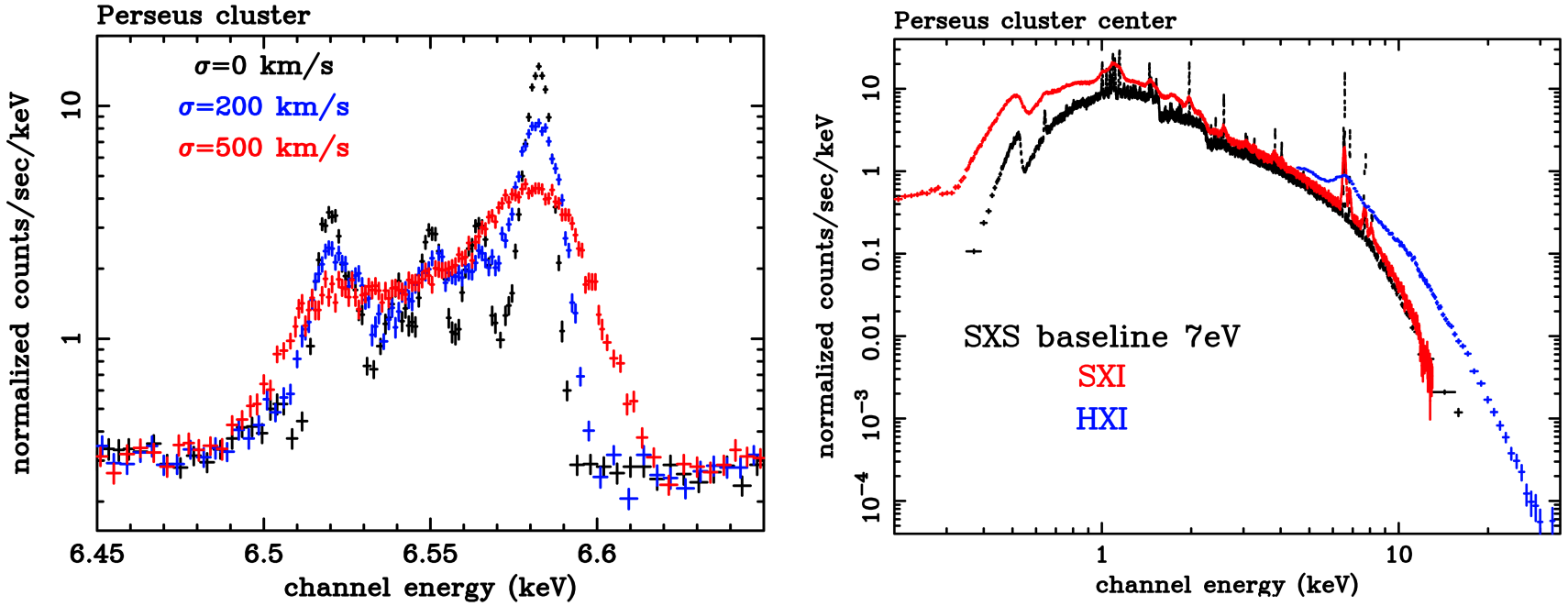

Simulated SXS spectra around the iron K line complex for 100 ks ASTRO-H observations of Perseus Cluster. Line profiles assuming σ=0, 100 and 200 km/s turbulence. Simulated broad-band spectra for hot plasma with three different temperatures of 0.6, 2.6 and 6. keV (Takahashi et al. 2010).

Summary

A very important synergy between the X-ray and VHE γ-ray observations of astrophysical sources of high energy radiation and particles with modern (future) instruments.

- **Low-Power Blazars (BL Lacs)**

probing particle acceleration with synchrotron X-rays and γ-rays

- **High-Power Blazars (FSRQs)**

probing jet energetic with inverse-Compton X-rays and γ-rays

- **Misaligned Blazars (Radio Galaxies)**

probing jet production with thermal X-rays and γ-rays

- **Radio-Quiet AGN (Seyferts)**

probing SMBH and accretion disk physics with X-rays and γ–rays

- **Cluster of Galaxies**

probing ICM dynamics and CR production with X-rays and γ–rays

- **All the Galactic sources… (SNRs, PWNe, XRBs, Sgr A*,…)**